ARTICLE

OPEN ACCESS

NPC1L1 on pancreatic adenocarcinoma cell functions as a two-pronged checkpoint against antitumor activity

Ruiyang Zi,[1,14] Kaicheng Shen,[2,14] Pengfei Zheng,[3,14] Xingxing Su,[4,14] Yishi Yang,[4] Yanrong Chen,[1] Haisu Dai,[4] Chengyi Mao,[5] Yongling Lu,[6] Liting Wang,[7] Hongbo Ma,[2] Wei Wang,[2] Qingyun Li,[8] Wei Lu,[9] Chengtao Li,[9] Shuangjia Zheng,[9] Hui Shi,[10] Xiaohong Liu,[11,*] Zhiyu Chen,[4,*] Houjie Liang,[1,*] and Juanjuan Ou[12,13,*]

*Correspondence: xiaohong.liu@nusricq.cn (X.L.); chenzhiyu_umn@163.com (Z.C.); lianghoujie@sina.com (H.L.); ojj521000@sina.com (J.O.)

Received: April 21, 2024; Accepted: December 30, 2024; Published Online: January 2, 2025; https://doi.org/10.1016/j.xinn.2024.100783

GRAPHICAL ABSTRACT

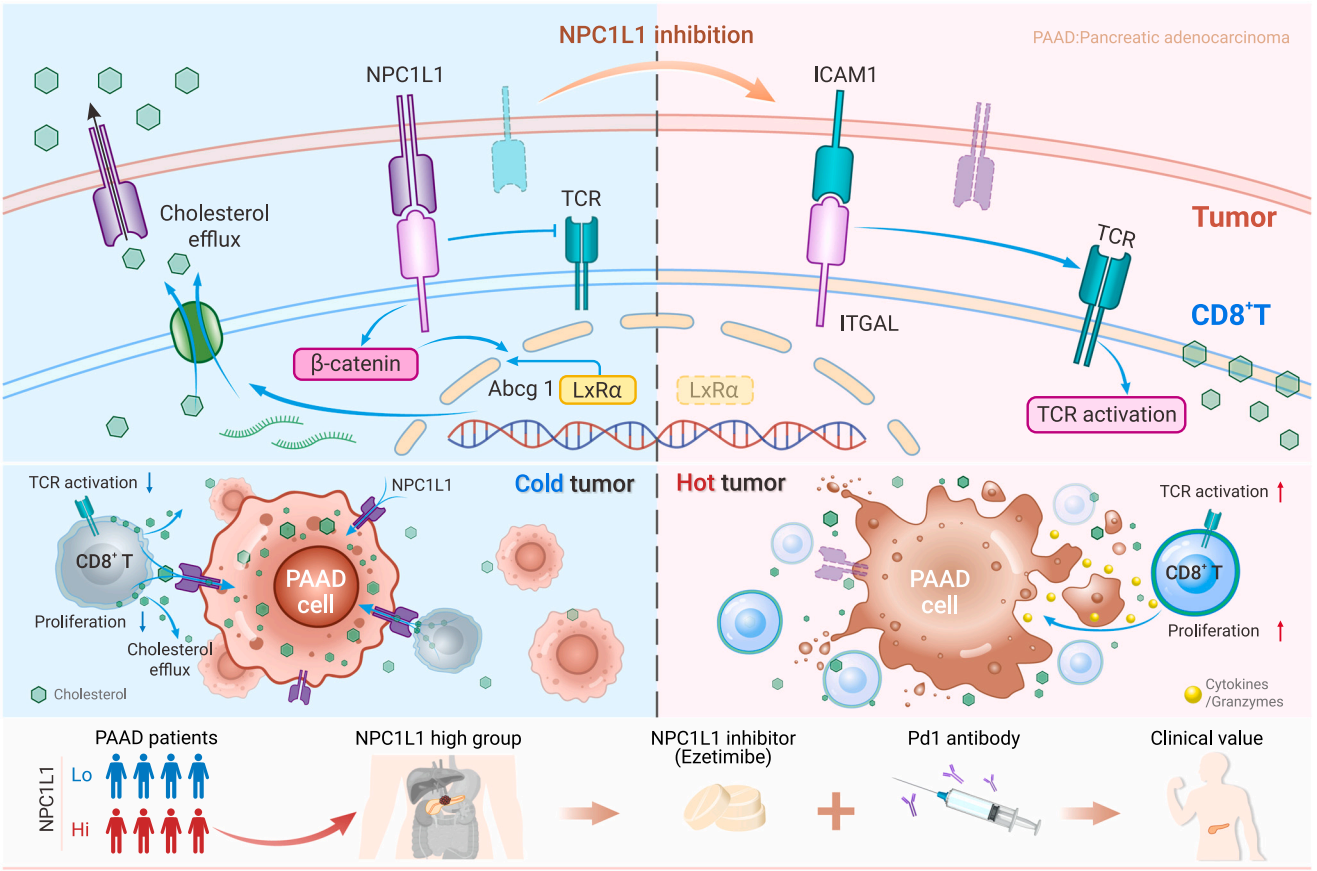

PUBLIC SUMMARY

- Pancreatic cancer cells overexpress NPC1L1 as a metabolic-immunologic checkpoint to outcompete CD8$^+$T cells.
- Cancer cells benefit by using NPC1L1 to hijack cholesterol from CD8$^+$T cells, impairing their function.
- Ezetimibe boosts CD8$^+$T cell responses and synergizes with PD-1 inhibitors to improve therapy outcomes.

OPEN ACCESS

ARTICLE

The Innovation

NPC1L1 on pancreatic adenocarcinoma cell functions as a two-pronged checkpoint against antitumor activity

Ruiyang Zi,[1,14] Kaicheng Shen,[2,14] Pengfei Zheng,[3,14] Xingxing Su,[4,14] Yishi Yang,[4] Yanrong Chen,[1] Haisu Dai,[4] Chengyi Mao,[5] Yongling Lu,[6] Liting Wang,[7] Hongbo Ma,[2] Wei Wang,[2] Qingyun Li,[8] Wei Lu,[9] Chengtao Li,[9] Shuangjia Zheng,[9] Hui Shi,[10] Xiaohong Liu,[11,*] Zhiyu Chen,[4,*] Houjie Liang,[1,*] and Juanjuan Ou[12,13,*]

[1]Department of Oncology and Southwest Cancer Center, Southwest Hospital, Third Military Medical University (Army Medical University), Chongqing 400038, China
[2]Department of Oncology, Fuling Hospital of Chongqing University, Chongqing 408000, China
[3]College of Pharmacy, Third Military Medical University (Army Medical University), Chongqing 400038, China
[4]Department of Hepatobiliary Surgery, Southwest Hospital, Third Military Medical University (Army Medical University), Chongqing 400038, China
[5]Department of Pathology, Daping Hospital, Third Military Medical University (Army Medical University), Chongqing 400042, China
[6]Medical Research Center, Southwest Hospital, Third Military Medical University (Army Medical University), Chongqing 400038, China
[7]Biomedical Analysis Center, Third Military Medical University (Army Medical University), Chongqing 400042, China
[8]Genecast Biotechnology Co., Wuxi 214104, China
[9]Galixir Technologies, Beijing 100086, China
[10]Department of Gastroenterology, The Second Medical Center & National Clinical Research Center for Geriatric Diseases, Chinese PLA General Hospital, Beijing 100853, China
[11]National University of Singapore (Chongqing) Research Institute, Chongqing 401123, China
[12]Yu-Yue Pathology Scientific Research Center, Chongqing 401329, China
[13]Center for Translational Research in Cancer, Sichuan Cancer Hospital & Institute, University of Electronic Science and Technology of China, Chengdu 610042, China
[14]These authors contributed equally
*Correspondence: xiaohong.liu@nusricq.cn (X.L.); chenzhiyu_umn@163.com (Z.C.); lianghoujie@sina.com (H.L.); ojj521000@sina.com (J.O.)

Received: April 21, 2024; Accepted: December 30, 2024; Published Online: January 2, 2025; https://doi.org/10.1016/j.xinn.2024.100783

Citation: Zi R., Shen K., Zheng P., et al., (2025). NPC1L1 on pancreatic adenocarcinoma cell functions as a two-pronged checkpoint against antitumor activity. The Innovation **6(3)**, 100783.

Pancreatic adenocarcinoma (PAAD) is a highly lethal malignancy with an immunosuppressive microenvironment and a limited immunotherapy response. Cholesterol is necessary for rapid growth of cancer cells, and cholesterol metabolism reprogramming is a hallmark of PAAD. How PAAD cells initiate cholesterol reprogramming to sustain their growth demand and suppressive immunomicroenvironment remains elusive. In this study, we for the first time revealed that PAAD cells overcome cholesterol shortage and immune surveillance via ectopically overexpressing NPC1L1, a cholesterol transporter, but function as a two-pronged checkpoint, which not only directly suppresses TCR activation of $CD8^+$T cells but also hijacks the intracellular cholesterol from $CD8^+$T cells. *In vivo*, we showed that ezetimibe, an NPC1L1 inhibitor usually for hypercholesterolemia, efficiently prevented PAAD cells from depriving cholesterol of $CD8^+$T cells, and improved the anti-tumor immunity of PAAD to synergize with PD-1 blockade, suggesting NPC1L1 as a promising target to rescue the anti-tumor activity in PAAD.

INTRODUCTION

$CD8^+$T cells play a critical role in anti-tumor immunity.[1] However, tumors can evade immune surveillance through diverse mechanisms of immunosuppression, one of which involves inhibiting the proliferation and activation of $CD8^+$T cells.[2] Recent evidence has demonstrated that reinvigorating the anti-tumor responses of $CD8^+$T cells by means of checkpoint inhibitors has shown remarkable therapeutic benefits in cancer treatment,[3–5] but not all cancers respond to checkpoint blockade. Pancreatic adenocarcinoma (PAAD), one of the deadliest human malignancies, infamously known for its refractoriness, presents substantial challenges to various forms of immunotherapy, encompassing treatments such as cytokine therapies, adoptive T cell transfer regimens, and even checkpoint inhibitor strategies.[6,7] The lack of success with these therapeutic modalities has been ascribed to $CD8^+$T cell scarcity or dysfunction and intense immunosuppression in the PAAD microenvironment.[8–10] Nonetheless, recent research has contested this prevailing notion and has revealed that a considerable number of pancreatic cancer patients indeed possess infiltrating T cells within their tumors alongside discernible neoantigens capable of eliciting potent T cell responses.[11–14] To design and refine therapies aimed at reviving T cell responses within pancreatic cancer, it is imperative to understand the underlying reasons that render endogenous T cell response ineffective in this setting.

Metabolic reprogramming is a well-established hallmark of cancer.[15,16] Tumor cells greatly disrupt tissue homeostasis, creating metabolically demanding environments that compete against the metabolic needs of infiltrating immune cells.[17] The uncontrolled cellular proliferation characteristic of cancer is frequently facilitated by aerobic glycolysis — a metabolic pathway that paradoxically also sustains the energy demands required for optimal effector functions in immune cells.[18,19] At a minimum, these similarities create competition for substrates between tumor cells and immune cells, which substantially limits the anti-tumor activity of immune cells.[20–22] In addition to glycolysis, lipids have long been recognized as an important aspect of the reprogrammed metabolism of cancer cells and are also important for immune cell function.[23] Cholesterol serves as a vital constituent of mammalian cell membranes critically attributable to the proliferation and T cell receptor (TCR) activation of $CD8^+$T cells.[24] Emerging evidence underscores the significance of cholesterol metabolism in maintaining and bolstering the cytotoxic capabilities of $CD8^+$T cells against tumor cells.[25] Epidemiological investigations have consistently demonstrated that individuals diagnosed with cancer often present with elevated plasma concentrations of lipoproteins, which serve as cholesterol transporters.[26,27] Concurrently, cancer cells exhibit dysregulated expression of multiple genes integral to cholesterol metabolism, including but not limited to the hydroxyl-methyl glutaryl-coenzyme A reductase (*HMGCR*), low-density lipoprotein receptor (*LDLR*), and sterol regulatory element-binding proteins (*SREBPs*).[26,27] While there is compelling evidence linking the reprogramming of cholesterol metabolism to carcinogenesis,[28] including its role in PAAD, the precise mechanisms by which tumors manipulate cholesterol metabolism to ensure their own survival and simultaneously dampen anti-tumor immune responses remain largely elusive.

In this study, we explored the novel and critical role of PAAD cell aberrantly and ectopically expressed NPC1L1, a cholesterol transporter normally expressed in the liver and small intestine, in suppressing anti-tumor $CD8^+$T cell activity in the PAAD tumor microenvironment, and the implication of NPC1L1 as a therapeutic target to rescue the anti-tumor immunity and improve the sensitivity of PAAD to immunotherapy.

MATERIALS AND METHODS

Materials and methods related to this study are available in the supplemental information.

Ethical statement and patient consent

All the experiments were performed in accordance with institutional guidelines and received ethical approval from the Animal Ethics Committee of Third Military Medical University.

RESULTS

A PAAD subtype with ectopic overexpression of NPC1L1 shows immunosuppressive microenvironment characterized with rare $CD8^+$T cell infiltration

Obesity and a high-fat diet are closely related to the development and progression of PAAD,[29] and we previously have found that hyperlipidemia is a hallmark of

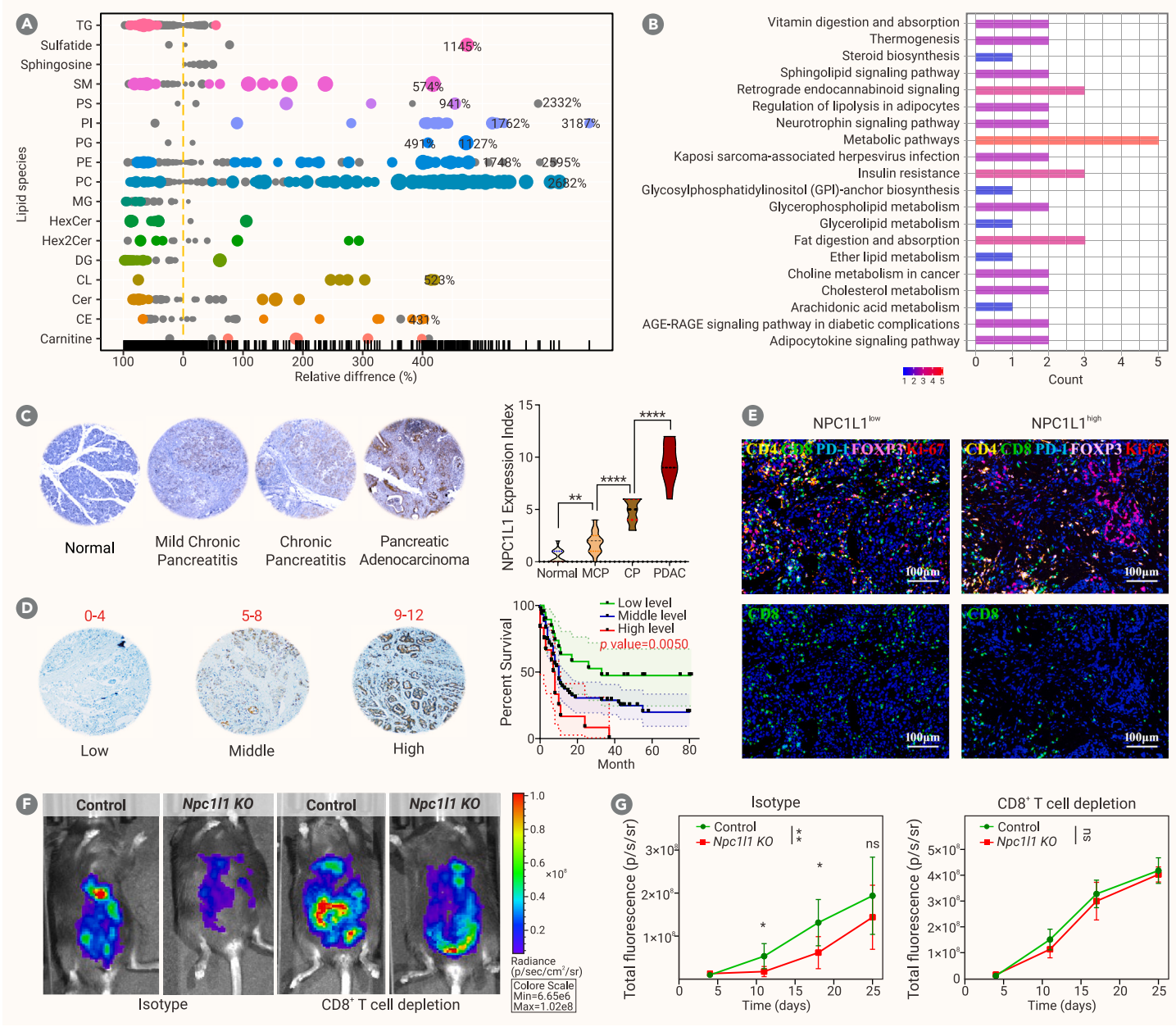

Figure 1. PAADs exhibit an ectopic overexpression of cholesterol transporter NPC1L1 accompanied with cholesterol addiction and suppressed CD8⁺T cell infiltration (A) Differentially expressed metabolites of lipidomic analyses between PAAD tumor tissues and adjacent pancreas tissues. Chemical similarity enrichment analysis for metabolites (ChemRICH) was conducted to calculate metabolite cluster statistics based on chemical similarities. These clusters are visualized by bubble plot. The y axis shows the most significantly altered lipid species, and the x axis shows the relative difference (%). *n* = 28 patients. (B) Kyoto Encyclopedia of Genes and Genomes (KEGG) pathway analysis of the differentially expressed proteins of proteomic analyses between PAAD tumor tissues and adjacent pancreas tissues. (C) Immunohistology (left) and quantification (right) of NPC1L1 expression in human pancreatic disease spectrum (pancreatic cancer progression) including normal pancreatic tissue, mild chronic pancreatitis, chronic pancreatitis, and PAAD. *n* = 13 patients per group. (D) Immunohistology of NPC1L1 expression of different scores in human primary PAAD tumors (left). Statistical analysis of the overall survival of PAAD subgroups with different NPC1L1 expression scores (score 0–4, mild; score 5–8, moderate; score 9–12, strong). (Kaplan-Meier survival curves) (right). *n* = 19, 59, 12 patients. (E) Representative mIHC images of NPC1L1-high and NPC1L1-low PAAD subgroups. (F) The representative IVIS images of C57BL/6J mice intraperitoneally inoculated with 10^6 *Npc1l1* KO or control Panc-02-luc allografts and treated with or without CD8⁺T cell-depleting antibody. (G) Tumor growth curves of C57BL/6J mice inoculated subcutaneously with 10^6 *Npc1l1* KO or control Panc-02 allografts and treated with isotype control (left) or depleting anti-CD8 (right) antibodies after inoculation for 5 days. Data represent 3 independent experiments with 8 mice per group. Error bars denote SEM. *p* values were calculated by ordinary one-way variance (ANOVA) in (H and G)and log rank test in (J). *$p < 0.05$, **$p < 0.01$, ****$p < 0.0001$; ns, no significance.

PAAD (Figure S1). Upregulation of lipoprotein and cholesterol metabolic pathways in PAAD has been reported. The authors showed increased total cholesterol, free cholesterol, and cholesteryl ester in PAAD compared with healthy pancreas, and demonstrated that blockade of cholesterol uptake by LDLR silencing reduces tumor growth.[30] By performing lipidomic analyses,[31] we found that lipids in 17 categories (sphingomyelin, glycerophosphatidylinositol, glycerophosphatidylserine, glycerophosphatidylglycerol, glycerophosphatidylethanolamine, glycerophosphatidylcholine, cardiolipin, and cholesterol esters) were at significantly higher levels in the PAAD tissues than in the adjacent pancreatic tissues ($p < 0.001$) (Figure 1A). We further examined the proteomic profile of PAAD tissue and adjacent pancreatic tissue by linear trap quadrupole-Orbitrap tandem mass spectrometry (MS/MS), and found that the cholesterol metabolism pathway was also enriched by the Gene Ontology (GO) enrichment analysis (Figure 1B). Impressively, by using Ingenuity Pathway Analysis of metabolites and proteins to identify the most top-ranked proteins attributable to the enriched cholesterol metabolites,[32,33] we found that NPC1L1, a cholesterol transporter responsible for cholesterol absorption normally expressed in intestine and liver, was ectopically and extremely highly expressed in PAAD relative to normal pancreas tissues (Figures S2A–S2C). To verify this, we analyzed single-cell transcriptome sequencing data from two pancreatic cancer cohorts (CRA001160

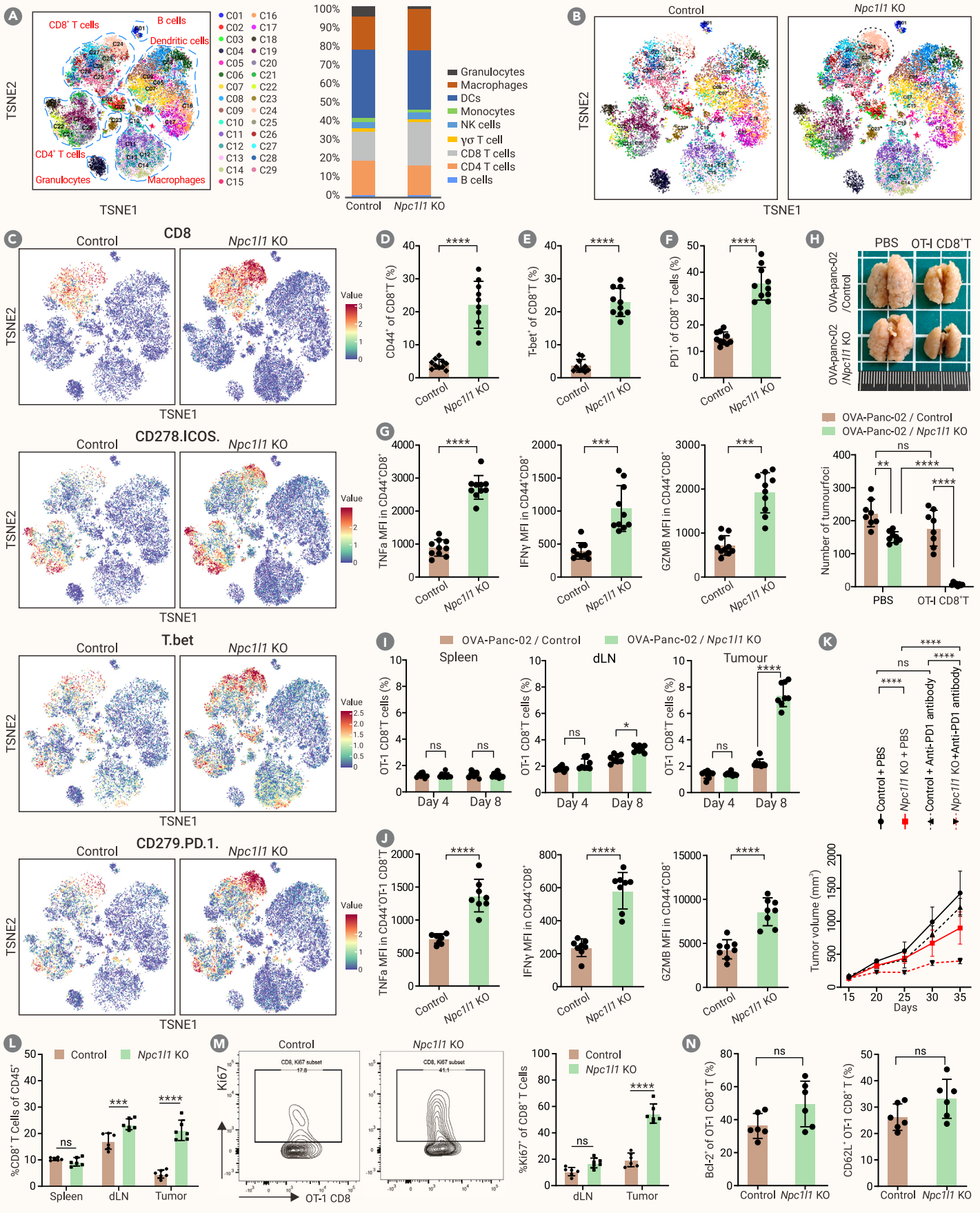

(legend on next page)

and GSE162708) in the database and found that NPC1L1 was indeed highly expressed only in pancreatic cancer cells and involved in regulating cholesterol homeostasis and cell-cell interaction while being virtually non-expressed in other stromal and immune cells (Figure S3). The integrated analyses of protein expression levels from proteomic profiles and mRNA expression levels from The Cancer Genome Atlas (TCGA)/Genotype-Tissue Expression confirmed that both the mRNA expression levels and protein expression levels of NPC1L1 were significantly increased in PAAD tissue relative to normal pancreatic tissue (Figure S2D). Meanwhile, the data from the Cancer Cell Line Encyclopedia also showed that most PAAD cell lines expressed abundant NPC1L1 (Figure S2E). As cancer cells display abnormal DNA methylation, which can lead to changes in the expression of tumor suppressor genes and oncogenes,[34,35] and increased expression of NPC1L1 at the mRNA level was found, we collected DNA methylation data for PAAD tissue samples from a TCGA cancer cohort. As expected, the NPC1L1 gene locus was extensively demethylated in PAAD (Figure S2F), and the mRNA expression levels of NPC1L1 were negatively correlated with the DNA methylation status (Figure S2G). We next separated the PAAD cohort into two groups based on the NPC1L1 DNA methylation status (high or low) with the corresponding (low or high, respectively) NPC1L1 mRNA expression level (Figures S2H and S2I) and found that the NPC1L1^{High}/methylation^{Low} status was associated with poor overall survival in PAAD patients (Figure S2J), indicating that, during PAAD carcinogenesis, the DNA methylation of NPC1L1 was decreased and the expression level of NPC1L1 was therefore increased. To further probe the relevance of NPC1L1 to PAAD pathogenesis, we next immunostained NPC1L1 in human PAAD tissues, and found that NPC1L1 was specifically expressed in PAAD cells but not in the stroma (Figure S2K). We further immunostained NPC1L1 in a tissue microarray containing a pancreatic disease spectrum (pancreatic cancer progression) including normal pancreatic tissue, mild chronic pancreatitis, chronic pancreatitis, and PAAD. As shown in Figure 1C, NPC1L1 expression levels were substantially increased in the PAAD samples versus the normal pancreas samples or benign pancreatic pathological alteration samples, and the expression of NPC1L1 was also found to be induced in the pancreatitis samples relative to normal pancreas samples. Importantly, higher NPC1L1 expression in PAAD tumors was associated with a lower diseased survival rate than lower NPC1L1 expression (Figure 1D). Collectively, this evidence strongly suggests a critical role of NPC1L1 in the development and progression of PAAD.

Nicoll et al. have described a subtype of PAAD (human xenograft model) with significant upregulation of cholesterol transporters including NPC1L1.[36] They reported that NPC1L1 high tumors show high levels of cholesteryl ester and a stromal upregulation of genes involved in lipid metabolism and cholesterol synthesis, and NPC1L1 inhibitor reduced tumor cell growth *in vitro* and *in vivo*.[36] Unlike LDLR, which is expressed in almost all tissues and organs of the body, NPC1L1 is specifically expressed in the liver and small intestine with little expression in pancreas. The dramatic upregulation of NPC1L1 in PAAD have been driving us to explore the potential role of NPC1L1 in PAAD pathogenesis. We then constructed *Npc1l1* knockout (KO) and *Npc1l1*-overexpressing murine PAAD cell lines with well used Panc-02 cells and KPC cells. The data from sequencing and PCR confirmed that *Npc1l1* has been successfully deleted or enforced (Figure S4). Notably, based on our verification, we found that all the commercial antibodies are not suitable for NPC1L1 immunoblotting (data not shown), but can be applied for NPC1L1 immunostaining. Expectedly, *Npc1l1* KO resulted in a suppression of cholesterol metabolism and cholesterol ester content (Figures S5A–S5C). Meanwhile, we found that *Npc1l1* KO decreased the proliferation and invasion capacity of PAAD cells (Figures S5D and S5F) and KPC cells (Figure S5I and S5J) but had little effect on cell apoptosis *in vitro* (Figure S5E). Very intriguingly, in allograft models, we found that the allografts established with *Npc1l1*-KO cells showed modestly decreased growth compared with the control group in nude mice (Figure S5G), while in C57BL/6 mice *Npc1l1*-KO allografts showed significantly decreased growth relative to control allografts in the early phase of tumorigenesis (Figure S5H). In addition, we confirmed the membrane localization of NPC1L1 in Panc-02 cells and KPC cells through immunofluorescence (Figure S5K). These findings strongly suggest a critical role of NPC1L1 in the regulation of anti-tumor immunity against PAAD.

To probe the immune signature related to NPC1L1 proficiency, we first analyzed a predefined immune signature matrix from the TCGA datasets[37,38] to estimate the fractions and abundances of tumor-infiltrating immune cell subsets (B cells, CD4$^+$T cells, CD8$^+$T cells, macrophages, neutrophils, and dendritic cells) in *NPC1L1*^{high} PAAD and *NPC1L1*^{low} PAAD. By six state-of-the-art algorithms, including TIMER, xCell, MCP-counter, CIBERSORT, and quanTIseq, we found that the relative number of infiltrating CD8$^+$T cells was significantly higher in the *NPC1L1*^{low} subgroup than in the *NPC1L1*^{high} subgroup, which is modestly shift between *LDLR*^{low} subgroup and *LDLR*^{high} subgroup (Figure S6A). Consistently, gene set enrichment analysis of TCGA PAAD dataset identified that the gene profiles of the inflammatory response were significantly enriched in *NPC1L1*^{low} PAAD (Figure S6B). We further conducted multiplex immunohistochemical (mIHC) analysis of 40 clinical PAAD samples and paired adjacent pancreatic tissue samples (Figure S6C). Immunocytes were more abundant in the tumor tissues than in the adjacent pancreatic tissues (Figures S6D and S6F), consistent with TCGA analysis results (Figures S6G and S6H). Impressively, the analyses of mIHC showed that the numbers of CD8$^+$, CD8$^+$PD-1$^+$, CD8$^+$Ki67$^+$, and CD8$^+$Ki67$^+$PD-1$^+$ cells both at the tumor margin and in the tumor center were significantly increased in the NPC1L1^{low} group compared with the NPC1L1^{high} group (Figures 1E, S6I, and S6J). This evidence indicated a potential role of highly expressed NPC1L1 in PAAD cells in suppressing tumor-infiltrated CD8$^+$T cells.

To examine the impact of NPC1L1 on the immune landscape, we further compared the immune infiltrates between control and *Npc1l1*-KO allografts by mass cytometry (CyTOF). More than 1.5 million immune cells were analyzed, and 29 subsets (clusters) were identified by cell surface markers for the total CD45$^+$ hematopoietic cell population (Figure S7A). In general, the immune landscape of *Npc1l1*-KO allografts was altered compared with that of control allografts and CD8$^+$T cells showed increased infiltrations in *Npc1l1*-KO allografts relative to that in control allografts (Figure 2A). To investigate whether the rise in the fraction of CD8$^+$T cells was indicative of a general increase in CD45$^+$ leukocytes infiltrating the tumors, we used GFP-expressing *Npc1l1*-KO and control Panc02 cells for *in vivo* studies. Flow cytometry was employed to enumerate the CD45$^+$ leukocytes and CD8$^+$T cells in relation to tumor cells within the allografts. This showed that *Npc1l1*-KO allografts indeed harbored a higher leukocyte-to-tumor cell ratio compared with controls, along with an elevated CD8$^+$T cell-to-tumor cell ratio (Figure S7B). However, there was no statistically significant difference observed in the ratio of CD4$^+$T cells to tumor cells (Figure S7C), and the proportion of regulatory T cells (FOXP3$^+$CD4$^+$T cells, or Tregs) within the total CD4$^+$T cells between *Npc1l1*-KO allografts and control allografts (Figure S7C). Consequently, this led to a higher ratio of CD8$^+$T cells to Tregs within the Npc1l1-KO allografts (Figure S7D). Moreover, we also evaluated the influence of NPC1L1 on other immune cell subsets. Specifically, it was found that natural killer (NK) cell numbers did not differ significantly between KO and control conditions (Figure S7E). Although the percentage of CD11b$^+$ myeloid cells is comparable between *Npc1l1*-KO and control allografts (Figure S7F), we observed a decreased

Figure 2. Highly expressed NPC1L1 on PAAD cells shows a potent role in suppressing the activity of tumor-specific CD8$^+$T cells (A and B) Phenograph of CD45$^+$ immune infiltrates overlaid with color-coded clusters from *Npc1l1* KO and control Panc-02 allograft CyTOF samples (pooled). (C) t-SNE plot of CD45$^+$ compartment overlaid with the expression of selected markers in *Npc1l1* KO and control Panc-02 allografts. (D–F) Flow cytometric analysis of tumor infiltrated CD8$^+$T cells from *Npc1l1* KO and control Panc-02 allografts. (D) T-bet$^+$CD8$^+$ double-positive cells (E) and PD-1$^+$CD8$^+$ double-positive cells (F) are shown (n = 10). (G) Cytokine/granule productions of tumor-infiltrated CD8$^+$T cells from *Npc1l1* KO and control Panc-02 allografts. (H–J) *Npc1l1* KO and control OVA-Panc-02 cells (1×10^6) were intravenously injected into C57 mice to induce lung allografts, and OT-1 CD8$^+$T cells were adoptively transferred to specifically target OVA-Panc-02 cells. (H) The representative gross images of dissected murine lung burdened with ectopic PAAD allografts, and tumor foci number of lung allografts in the indicated groups were counted and analyzed (n = 8). (I) Frequency of OT-1 CD8$^+$T cells as a percentage of CD45$^+$ cells in spleen, tumor-draining lymph node (TDLN), and tumor. (J) IFN-γ, TNF-α, and GzmB expression in OT-1 CD8$^+$T cells from spleen, TDLN and tumor. MFI, mean fluorescence intensity. (K) Tumor growth curves of C57BL/6J mice subcutaneously inoculated with 10^6 *Npc1l1* KO or control OVA-Panc-02 cells and treated with PBS or anti-PD-1 antibodies 10 mg/kg twice a week after inoculation for 10 days (n = 6). (L) The quantification of OT-1 CD8$^+$T cell to CD45$^+$ cell ratio in spleen, TDLN, and tumor (n = 6). (M) Quantification of Ki67 expression among OT-1 CD8$^+$T cells in tumor (n = 6). (N) Quantification of Bcl-2 and CD62L expressions among OT-1 CD8$^+$T cells in tumor (n = 6). Error bars denote SEM. p values were calculated by unpaired two-tailed t test in (D–G), (I and J), and (L–N). Statistical significance was assessed by two-way ANOVA with Tukey's multiple comparisons test in (H) and (K). *p < 0.05, **p < 0.01, ***p < 0.001, ****p < 0.0001; ns, not significant.

proportion of GR1$^+$CD11b$^+$ myeloid-derived suppressor cells (Figure S7G) and increased proportion of F4/80$^+$GR1$^-$CD11b$^+$ macrophages (TAMs) (Figure S7H). We also examined the presence of CD11c$^+$ dendritic cells, which are recognized for their ability to activate T cells by presenting antigens. Upon analysis, the percentage of CD11c$^+$ dendritic cells in *Npc1l1*-KO allografts was similar to that in control allografts (Figure S7I). Based on the data presented, it appears that the KO of Npc1l1 has a significant effect on the composition of immune cells within the tumor microenvironment, particularly influencing the CD8$^+$T cell population. To further determine whether CD8$^+$T cells play the dominant role in mediating the effect of NPC1L1 on PAAD growth, we applied CD8$^+$T cell-depleting antibody to the allograft models. Expectedly, CD8$^+$T cell depletion substantially abolished the shift of early allograft growth between control and *Npc1l1*-KO groups (Figures 1F and 1G), further supporting the critical role of CD8$^+$T cells in mediating the effect of NPC1L1 on PAAD tumor growth.

PAAD cells express NPC1L1 to suppress the activation and proliferation of anti-tumor CD8$^+$T cells in the tumor microenvironment

Notably, the analyses of CyTOF have found that, in the *Npc1l1*-KO allografts, the subcluster proportion of CD8$^+$T cells, especially that of cluster 24, was dramatically increased (336%) (Figures 2A and 2B). The CD8$^+$T cells in cluster 24 showed enhanced expressions of T-bet, ICOS, and PD-1 (Figure 2C). T-bet is thought to be an important transcription factor of stem-like CD8$^+$T cells that can respond to PD-1 blockade and enhance the anti-tumor response,[39,40] suggesting the enhanced function of anti-tumor CD8$^+$T cells in *Npc1l1*-KO allografts. Consistently with CyTOF analysis, our FACS data also showed that CD8$^+$T cell population in *Npc1l1*-KO tumors presented increased frequencies of cells expressing CD44, T-bet, and PD-1 relative to that in control tumors (Figures 2D–2F). Meanwhile, the CD44$^+$CD8$^+$T cells from *Npc1l1*-KO allografts produced more IFN-γ, TNF-α, and GZMB than those from control tumors upon restimulation *in vitro* (Figure 2G), indicating their development of effector characteristics.

To determine whether these effector-phenotype cells are relevant to the anti-tumor response, we next established OVA-expressing *Npc1l1*-KO or control Panc-02 cells (OVA-Panc-02) and established lung allografts via tail vein injection, and treated allograft mice with OT-I CD8$^+$T cell adoptive transfer supplemented with interleukin-2 (IL-2) 7 days after allograft inoculation and recovered lymphoid tissues and tumors 4 and 8 days later to assess their frequency and activity. As expected, lung allografts were efficiently suppressed in the *Npc1l1*-KO group by OT-I CTLs (Figure 2H). In both control and *Npc1l1*-KO allograft mice, the spleen contained small numbers of OT-I CTLs at days 4 and 8 (Figure 2I). In tumor-draining lymph nodes (dLNs), we detected a modest increase in the frequency of OT-I CD8$^+$T at days 4 and 8 in *Npc1l1*-KO allograft mice relative to those in control allograft mice (Figure 2I). Impressively, the frequency of OT-I CD8$^+$T were significantly increased in *Npc1l1*-KO allograft tumors in comparison with control tumors (Figure 2I). Meanwhile, we found that tumor OT-I CD8$^+$T from *Npc1l1*-KO group 8 days after cell transfer expressed significantly increased levels of IFN-γ, TNF-α, and GMZB compared with those in the control group (Figure 2J). Thus, the *Npc1l1*-KO-induced accumulation of CD8$^+$T cells in the tumor microenvironment is not an expansion of irrelevant T cell clones but rather the accumulation of tumor-specific effector CD8$^+$T cells with direct tumor-targeting potential. Expectedly, the response of *Npc1l1*-KO allografts to anti-PD-1 antibody treatment was significantly more robust than that of control allografts (Figure 2K).

Importantly, we also observed that the increase of the percentage of OT-I CD8$^+$T to total CD45$^+$ cells was specific to the tumor, but not in the spleen or dLNs (Figure 2L). We next sought to determine whether the increased OT-I CD8$^+$T cells in *Npc1l1*-KO allografts are likely to have arisen from the priming of naive anti-tumor T cells or the expansion of T cells primed in the lymph nodes (LNs). Impressively, while the frequency of Ki67$^+$ OT-I CD8$^+$ cells in the dLNs was modestly increased in *Npc1l1*-KO group relative to that in control group, the frequency of Ki67$^+$ OT-I CD8$^+$T cells in tumors was significantly increased in comparison with that in control tumors (Figure 2M). The frequency of Ki67$^+$ OT-I CD8$^+$ cells in the dLNs did not predict the frequency of tumor-resident Ki67$^+$ OT-I CD8$^+$ cells: the *Npc1l1*-KO group uniformly exhibited large increases in the tumor-infiltrated CD8$^+$T cell population than in tumor-dLNs. Since the tumor-infiltrated T cell number is determined by the balance among the proliferation, exhaustion-associated apoptosis, and homing of CD8$^+$T cells to the secondary lymphoid organs,[41] we further investigated whether *Npc1l1* KO in PAAD cells can affect the apoptosis or homing of CD8$^+$T cells. FACS analyses showed that the percentage of Bcl-2$^+$ OT-I CD8$^+$T cells in *Npc1l1*-KO tumors was relatively unchanged compared with that in control tumors (Figure 2N). Meanwhile, the homing receptor CD62L between *Npc1l1*-KO and control allografts were also comparable between OT-I CD8$^+$T cells sorted from *Npc1l1*-KO allografts and those sorted from control allografts (Figure 2N). Thus, silencing *Npc1l1* in PAAD cells appears to enhance the CD8$^+$T cell proliferation and activation capacity mainly at a post-LN stage, possibly in the tumor site while exerting only modest effects on CD8$^+$T cell priming, apoptosis, and homing.

NPC1L1 overexpression promotes PAAD cells to evade CD8$^+$T cell immunosurveillance and is responsible for *de novo* PAAD development

Since the studies utilizing orthotopic or heterotopic tumor grafts models may not fully replicate the natural progression of PAAD and have very divergent immune contexture.[42] The "KPC" (Kras+/LSL-G12D; Trp53 fl/fl; Pdx1-Cre) mouse model is a widely adopted genetically engineered model for studying pancreatic ductal adenocarcinoma (PDAC), which closely mirrors the characteristics of human patients, notably activating mutations in Kras (G12D) and loss of Trp53, associated desmoplasia, and inflammation.[43,44] The model also mirrors human disease in its resistance to both cytotoxic and immunotherapies.[45,46] To examine the impact of NPC1L1 on tumor immunity in the context of *de novo* PDAC development, we established a KPC model and selectively silenced *Npc1l1* in the pancreas via tail vein injecting adeno-associated virus (AAV) expressing shNpc1l1 under control of the pdx-1 promoter (AAV-pdx1-shNpc1l1-GFP, referred to as AAV-shNpc1l1) into KPC mice, while injecting AAV-pdx1-shScrmbl-GFP (AAV-shScrmbl) control virus to control mice (Figure S8A). The knockdown efficiency of AAV-shNpc1l1 in the pancreas was confirmed through qPCR (Figure 3A) and immunohistochemistry (Figure S8B). In control KPC mice, malignant lesions have emerged in KPC mice at 24 weeks, and *Npc1l1* silencing led to marked decreases in late-stage intraepithelial neoplasia (PANIN) lesions and malignant tumor formation (Figures 3A–3C), associated with a decreased collagen deposition, proliferation index (Figures S8C and S8D), and prolonged overall survival (Figure 3D). Meanwhile, we found that *Npc1l1* silencing showed little effect on mouse body weight and plasma cholesterol level (Figures S8E–S8G).

Consistent with the hypothesis, we observed a significant enhancement in the quantity of CD8$^+$T cells in the pancreas of AAV-shNpc1l1-KPC compared with AAV-shScrmbl-KPC mice with CD8$^+$T cells modestly increased in dLNs and comparable numbers of CD8$^+$T cells in spleens (Figure 3E). Interestingly, upon comparing the CD8$^+$T cells found in the pancreas of AAV-shNpc1l1-treated KPC mice with those in control animals, it was discovered that the CD8$^+$T cells in the former group exhibited a higher frequency of CD44 expression, and >15% of them were PD-1$^+$, suggesting an active phenotype (Figure 3F). Consistent with that in allograft models, analysis of the inflammatory infiltrates indicated a comparable infiltration of CD4$^+$ and Foxp3$^+$CD4$^+$ cells in the pancreas of AAV-shNpc1l1-KPC relative to AAV-shScrmbl-KPC mice (Figure 3G). Meanwhile, we observed increased macrophages and a decreased infiltration of granulocytes, while little shift of monocytes in the pancreas of AAV-shNpc1l1-KPC relative to AAV-shScrmbl-KPC mice (Figure 3H). Meanwhile, little shift of plasma glucose and plasma IL-6 level was observed between AAV-shNpc1l1-KPC and AAV-shScrmbl-KPC mice (Figures S8H and S8I). Collectively, this evidence further supports that NPC1L1 silencing improves the anti-tumor immunity, specifically in the tumor microenvironment, rather than promoting systemic immunity.

Since previous studies have shown that CD4$^+$T cells can drive pathogenic inflammation and accelerate PDAC progression,[47–51] we further evaluated whether CD4$^+$ or CD8$^+$T cells were predominantly attributable for NPC1L1-induced pathogenesis. We found that, while CD4$^+$T depletion did not alter malignant lesion progression, CD8$^+$T cell depletion substantially reversed the malignant lesion burden and collagen density in the pancreas of AAV-shNpc1l1-KPC to the extent of AAV-shScrmbl-KPC mice (Figure 3I).

Since chronic pancreatic inflammation is strongly associated with pancreatic cancer,[52,53] to determine whether NPC1L1 also affects the activity of CD8$^+$T cells in chronic pancreatitis, we established a C57 mouse model with constitutive knockin of *Npc1l1* under control of the *Pdx1* promoter (*Npc1l1*^{pdx1} mice) and

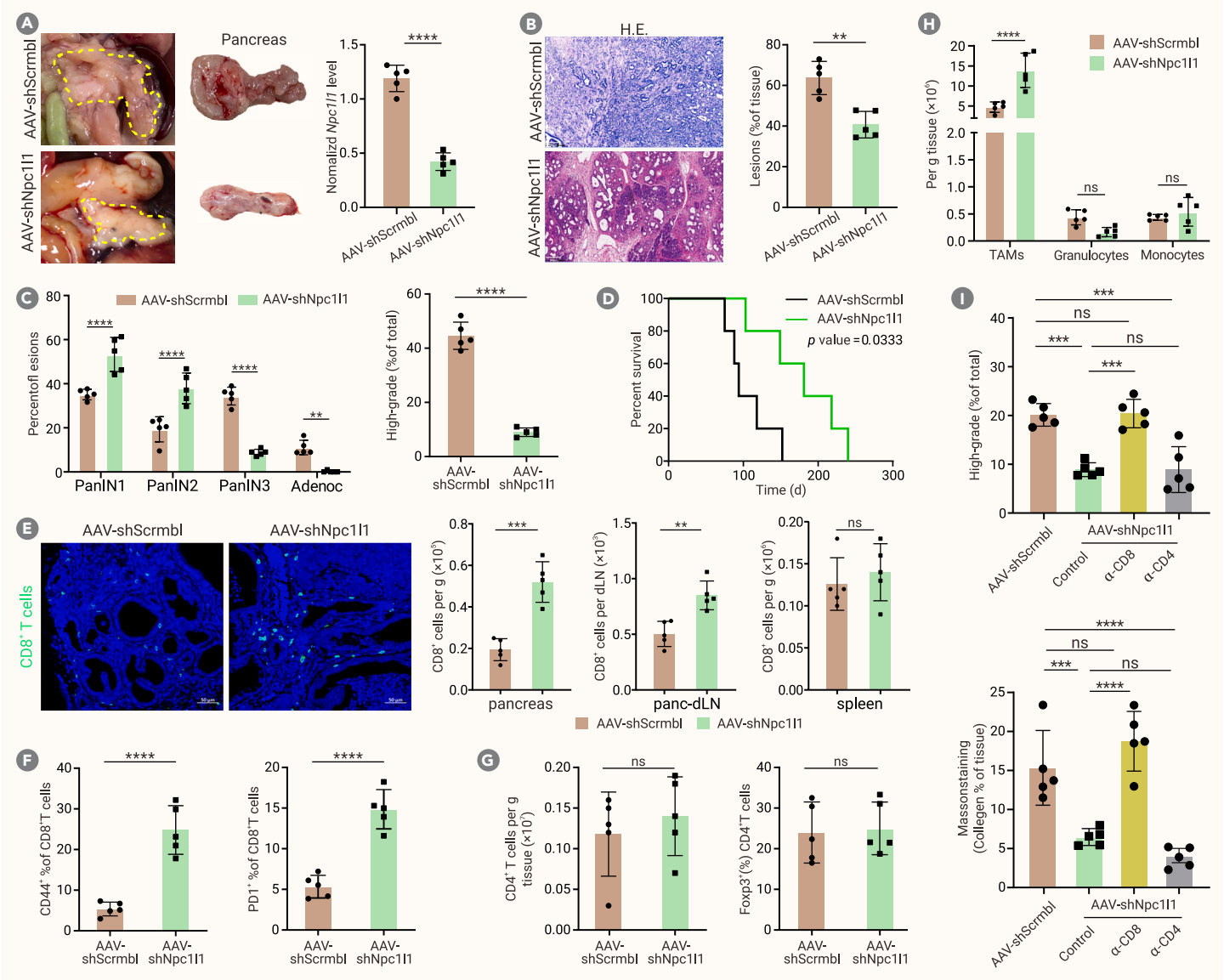

Figure 3. NPC1L1 promotes *de novo* PDAC development (A) Gross images and Npc1l1 mRNA expression level of pancreatic tissue in AAV-shScrmbl- or AAV-Npc1l1-treated KPC mice at age 24 weeks. (B) Representative hematoxylin and eosin (H&E) images with quantification of lesions in pancreatic tissue in AAV-shScrmbl- or AAV-Npc1l1-treated KPC mice at age 24 weeks. n = 5 mice/group. Scale bars, 200 μm. (C) Lesion grades for pancreatic tissue in AAV-shScrmbl- or AAV-Npc1l1-treated KPC mice at age 24 weeks. n = 5 mice/group. (D) Kaplan-Meier survival curve for KPC mice treated with AAV-shScrmbl or AAV-Npc1l1. n = 5 mice/group. (E) Representative immunofluorescent staining of $CD8^+$T cells with quantification of the density of $CD8^+$T cells in pancreatic tissue, dLN, and spleen at 24 weeks in KPC mice treated with AAV-shScrmbl or AAV-Npc1l1. n = 5 mice/group. Scale bars, 200 μm. (F) Quantification of $CD44^+CD8^+$ and $PD1^+CD8^+$T cells in pancreatic tissue of AAV-shScrmbl- or AAV-Npc1l1-treated KPC mice at age 24 weeks. n = 5 mice/group. (G) Density of $CD4^+$T cells and Foxp3$^+$ $CD4^+$T cells measured by flow cytometry in pancreatic tissue of AAV-shScrmbl- or AAV-Npc1l1-treated KPC mice at age 24 weeks. n = 5 mice/group. (H) Flow-cytometric quantification of various myeloid infiltrates in pancreatic tissue in AAV-shScrmbl- or AAV-Npc1l1-treated KPC mice at age 24 weeks. n = 5 mice/group. (I) Lesion grades and Masson staining with quantification in pancreatic tissue in AAV-shScrmbl- or AAV-Npc1l1-treated KPC mice subjected to indicated depletions at age 4 weeks. n = 5 mice/group. Error bars denote SEM. p values were calculated by unpaired two-tailed t test in (B), (C, right), and (E–G). Statistical significance was assessed by two-way ANOVA with Tukey's multiple comparisons test in (C, left), (H), and (I). (D) Analyzed with log rank test. $^{**}p < 0.01$, $^{***}p < 0.001$, $^{****}p < 0.0001$; ns, no significance.

established a chronic pancreatitis model by intraperitoneally injecting arginine (Figure S9A). Intriguingly, we found that, in *Npc1l1*^{pdx1} mice with pancreatitis, the infiltrating $CD8^+$T cells in the pancreas tissue showed comparable proliferation and cytotoxic activity relative to those in wild-type mice with chronic pancreatitis (Figures S9B and S9C). This evidence suggests that the NPC1L1 may exert its inhibitory effect on $CD8^+$T cells only in the context of PAAD tumorigenesis but not in a simple inflammation status. Our observations from *de novo* pancreas cancer models mirror our allograft mouse models, further supporting a critical role of NPC1L1 in suppressing the activation and proliferation of $CD8^+$T cells in PAAD.

NPC1L1 impairs tumor-specific $CD8^+$T cell activity and expansion in a cell-cell interaction manner

To explore how NPC1L1-proficient PAAD cells impede the anti-tumor activity and proliferation of $CD8^+$T cells in the tumor microenvironment, we mimicked the tumor microenvironment by coculturing OVA-Panc-02 cells with OT-I $CD8^+$T cells primed with α-CD3/CD28 stimulation. Impressively, T cell killing assays showed that OVA-specific OT-I $CD8^+$T cells effectively killed *Npc1l1*-KO OVA-Panc-02 cells but showed little effect on control OVA-Panc-02 cells (Figures 4A and 4B). Under the monitoring of the living cell workstation, we observed an efficient killing by OT-I $CD8^+$T cells against *Npc1l1*-KO OVA-Panc-02 cells but not control OVA-Panc-02 cells (Figure 4C; Videos S1 and S2). The same phenomenon was also observed in the OVA-KPC cells under confocal microscope (Figure 4D; Videos S3 and S4). By electron microscopy, direct contact between OT-I $CD8^+$T cells and tumor cells was observed both in *Npc1l1*-KO OVA-Panc-02 and control OVA-Panc-02 groups. Very impressively, while the *Npc1l1*-KO OVA-Panc-02 cells contacted with OT-I $CD8^+$T cells showing a dying phenotype characterized with cell swelling and bubbling, most of the control OVA-Panc-02 cells were intact and proliferative (Figure 4E). Meanwhile, unlike those OT-I $CD8^+$T cells contacting with *Npc1l1*-KO OVA-Panc-02 cells, which look plump and full of rigidity, the OT-I $CD8^+$T cells contacting with control OVA-Panc-02 cells were losing their stiffness and showing

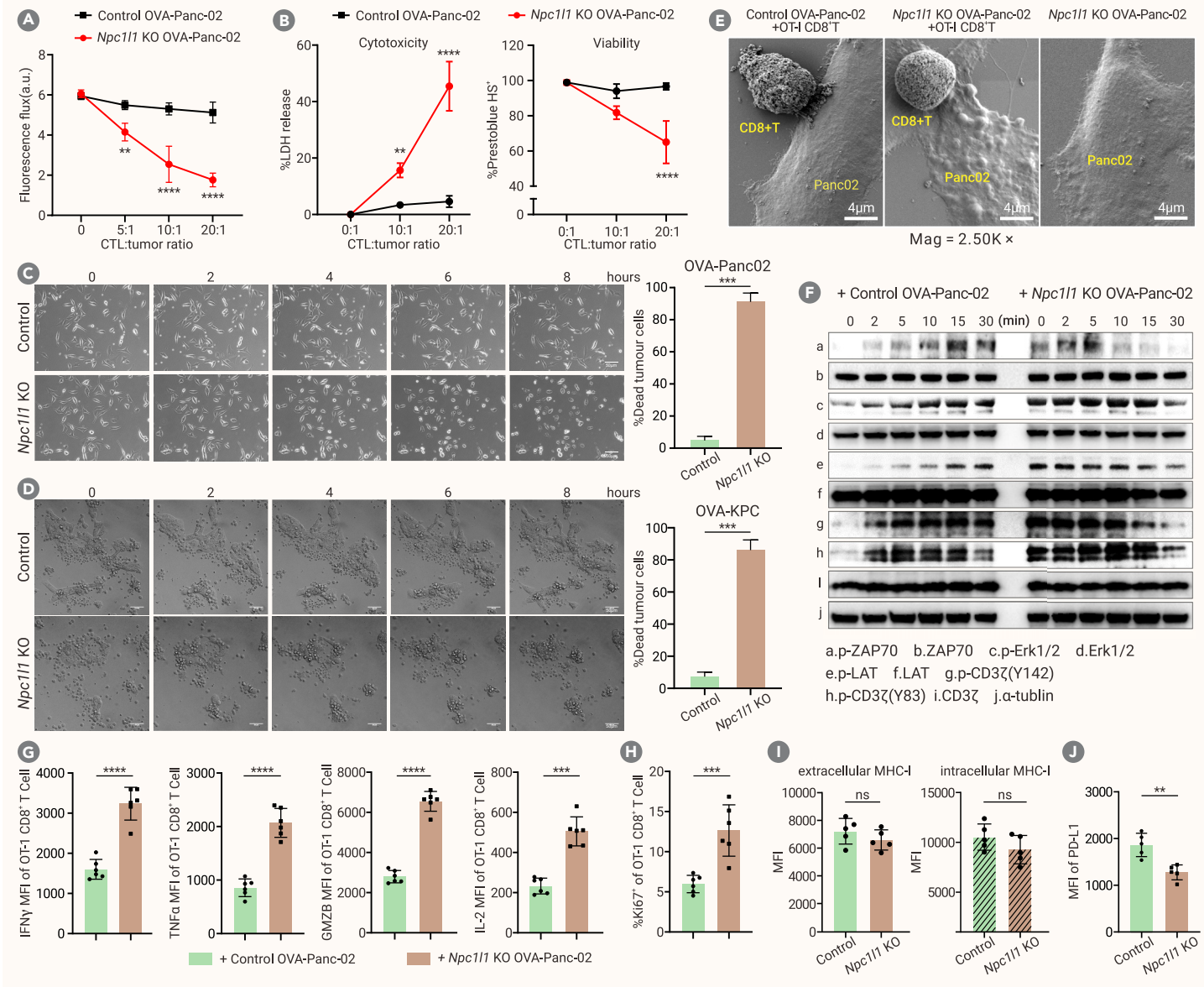

Figure 4. NPC1L1 on PAAD cells inhibits TCR activation and cytotoxicity of anti-tumor CD8$^+$T cells (A) *Npc1l1* KO and control OVA-Panc-02 cells depicting GFP fluorescence after 24-h coculture with antigen-specific (OT-I TCR) activated CD8$^+$T cells (CTL) under indicated CTL: tumor cell ratio. *n* = 3/group. (B) *In vitro* LDH release and resazurin-based viability of *Npc1l1* KO and control OVA-Panc-02 cells after 72-h coculture with activated antigen-specific (OT-I TCR) CD8$^+$T cells. *n* = 3/condition. (C) The representative images of *Npc1l1* KO and control OVA-Panc-02 cells cocultured with OT-I CD8$^+$T cells at the indicated time points. Tumor cells with a 50% reduction in either their long or short diameter are considered to be dead (*n* = 6). (D) The representative confocal images of *Npc1l1* KO and control OVA-KPC cells cocultured with OT-I CD8$^+$T cells at the indicated time points. Tumor cells with a 50% reduction in either their long or short diameter are considered to be dead (*n* = 6). (E) Representative electron microscopic images depicting the interactions between OT-I CTLs and *Npc1l1* KO or control OVA-Panc-02 cells. (F) TCR proximal and downstream signaling was assessed using immunoblotting of protein phosphorylation. OT-I CTLs were cocultured with *Npc1l1* KO or control OVA-Panc-02 cells for the indicated time. (G) Mean fluorescence intensity of the indicated markers in OT-I CTLs cocultured with *Npc1l1* KO or control OVA-Panc-02 cells. (H) Quantification of Ki67 expression among OT-1 CTLs cocultured with *Npc1l1* KO or control OVA-Panc-02 cells. (I) Mean fluorescence intensity of extracellular MHC-I expression in *Npc1l1* KO and control OVA-Panc-02 cells. *n* = 5 lines each. (J) Mean fluorescence intensity of PD-L1 expression in *Npc1l1* KO and control OVA-Panc-02 cells. *n* = 5 lines each. Error bars denote SEM. *p* values were calculated by unpaired two-tailed t test in (E)–(J) and two-way ANOVA with Tukey's multiple comparisons test in (A) and (B). $^{**}p < 0.01$, $^{***}p < 0.001$, $^{****}p < 0.0001$; ns, no significance.

a collapsed cell membrane instead (Figure 4E). These phenotypes strongly indicate a life-or-death struggle between PAAD cells and CD8$^+$T cells, and NPC1L1 provides the absolute superiority of PAAD cells in fighting against CD8$^+$T cells. As expected, TCR signaling, a major signal controlling T cell activation and proliferation, was significantly enhanced in OT-I CD8$^+$T cells cocultured with *Npc1l1*-KO OVA-Panc-02 cells compared with those in the control group (Figure 4F), and OT-I CD8$^+$T cells cocultured with *Npc1l1*-KO OVA-Panc-02 cells expressed more GZMB, IFN-γ, and TNF-α (Figure 4G), accompanied with increased IL-2 production (Figure 4G), and were more proliferative, based on Ki67 levels (Figure 4H). Since major histocompatibility complex 1 (MHC-I) and PD-L1 are well-known factors determining the cytotoxicity efficacy of tumor-specific effector CD8$^+$T cells to contacting cancer cells, we compared the expression levels of MHC-I and PD-L1 between *Npc1l1*-KO and control OVA-Panc-02 cells. Intriguingly, we found that *Npc1l1*-KO did not alter the expression of MHC-I and just modestly decreased the expression level of PD-L1 (Figures 4I and 4J), indicating that NPC1L1 may regulate the activation and proliferation of tumor-specific effector CD8$^+$T cells via a pathway parallel to MHC-I and PD-L1.

NPC1L1 helps PAAD cells to outcompete against CD8$^+$T cells for exogenous cholesterol uptake and hijack the intracellular cholesterol of anti-tumor CD8$^+$T cells via promoting β-catenin-LXR-induced cholesterol efflux from CD8$^+$T cells

To further elucidate the exact molecular mechanism by which NPC1L1 profoundly influences the activity and proliferation of tumor-specific CD8$^+$T cells within the tumor microenvironment, subsequent experiments were executed. Cholesterol is a crucial element in the structure and function of cellular membrane and has been shown to be needed for T cell proliferation, TCR clustering,

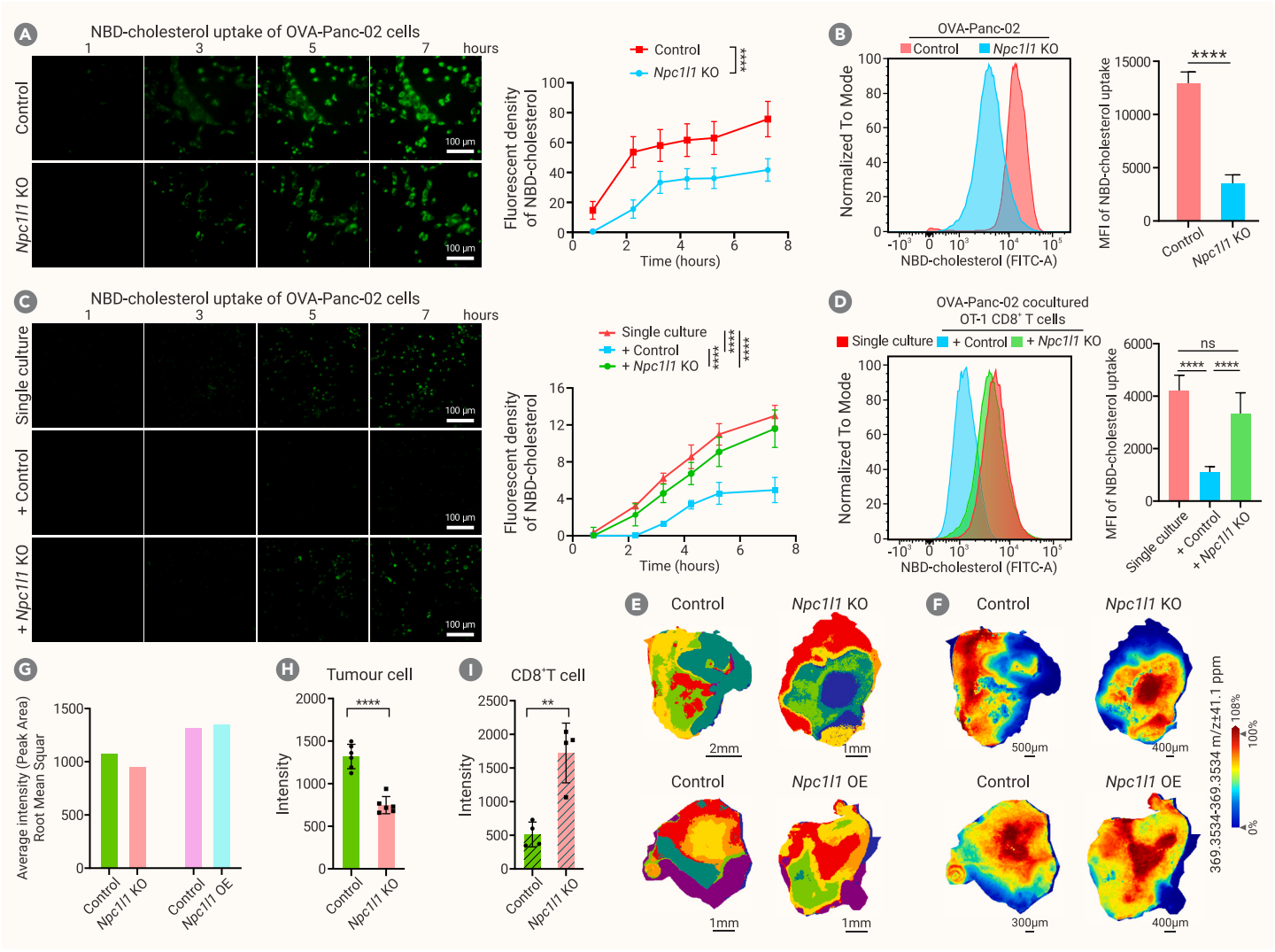

Figure 5. NPC1L1 helps PAAD cells to outcompete the cholesterol from microenvironment and hijack the intracellular cholesterol from anti-tumor CD8$^+$T cells (A) *Npc1l1* KO and control OVA-Panc-02 cells were cultured in complete medium supplemented with 20 μM NBD-cholesterol. Representative images depicting the NBD immunofluorescence in *Npc1l1* KO and control OVA-Panc-02 cells at the indicated time point, and the fluorescence intensity was calculated by ImageJ software (n = 5). (B) Representative FACS graphs (left) and statistical analysis (right) of mean fluorescence intensity of NBD immunofluorescence in *Npc1l1* KO and control OVA-Panc-02 cells (n = 5). (C and D) OT-I CTLs were single cultured or cocultured with *Npc1l1* KO/control OVA-Panc-02 cells (0.1 μM NBD-cholesterol was added in medium). For cocultured OT-I CTLs, OT-I CTLs at indicated time point were rinsed off for image shooting. Representative images depicting the NBD immunofluorescence in OT-I CTLs at the indicated time point (C). Representative FACS graphs (left) and statistical analysis (right) of mean fluorescence intensity of NBD immunofluorescence in OT-I CTLs as shown (D) (n = 5). (E) Segmentation map of MALDI MSI data produced via bisecting k-means clustering (k = 8), whereby different clusters were labeled with different colors, and separate clusters are indicated within the tumor region, indicating spectral differences between these regions. (F) MALDI MSI ion images of cholesterol in tumor slices from *Npc1l1* KO/control OVA-Panc-02 cells and *Npc1l1*-overexpressing/control OVA-Panc-02 allografts. (G) Graphs depicting average (mean) ion intensity of cholesterol (m/z 369.3534) in the indicated groups. (H) Graphs depicting ion intensity of cholesterol (m/z 369.3534) of the delineated tumor cell area in the tumor slices of *Npc1l1* KO and control allografts. (I) Graphs depicting ion intensity of cholesterol (m/z 369.3534) of the delineated CD8$^+$T cell area in the tumor slices of *Npc1l1* KO and control allografts. Error bars denote SEM. p values were calculated by unpaired two-tailed t test in (E), (H), and (I). Statistical significance was assessed by two-way ANOVA with Tukey's multiple comparisons test in (A) and (C). (D) Analyzed by ordinary one-way variance (ANOVA) with Tukey's multiple comparisons test. $^{**}p < 0.01$, $^{****}p < 0.0001$; ns, no significance.

and T cell immunological synapse formation,[54–58] and previous studies have demonstrated that the anti-tumor response mediated by CD8$^+$T cells can be augmented by manipulating cholesterol metabolism.[25] Since NPC1L1 is a transporter for cholesterol uptake,[36] we speculated that NPC1L1 may help PAAD cells to competitively uptake cholesterol from the tumor microenvironment against CD8$^+$T cells, which leads to their dysfunction. As expected, in a cholesterol loading assay, *Npc1l1*-KO OVA-Panc-02 cells exhibited a significantly decreased uptake rate and level of exogenous 25-NBD cholesterol compared with control cells (Figures 5A and 5B), and *Npc1l1*-overexpressing OVA-Panc-02 cells showed increased cholesterol uptake capacity relative to control cells (Figure S9D). Similar phenomena were copied by *Npc1l1*-KO and *Npc1l1*-overexpressing OVA-KPC cells (Figure S10; Videos S5, S6, S7, and S8). Meanwhile, we found that, under the culture condition with limited exogenous cholesterol, the cholesterol uptake of OT-I CD8$^+$T cells cocultured with control OVA-Panc-02 cells was significantly decreased relative to those single cultured, and this effect was abolished when cocultured with *Npc1l1*-KO OVA-Panc-02 cells (Figures 5C and 5D), suggesting that NPC1L1 may help PAAD cells to outcompete against CD8$^+$T cells for cholesterol uptake from the tumor microenvironment.

To further confirm the NPC1L1-induced competition of cholesterol between tumor cells and CD8$^+$T cells in the tumor microenvironment, we conducted the allografts derived from *Npc1l1*-KO, *Npc1l1*-overexpressing, and control OVA-Panc-02 cells for spatial lipid metabolomic analysis. As shown in Figure S11A, the pattern of lipid metabolites detected by mass spectrometry exhibited little shift between *Npc1l1*-manipulated OVA-Panc-02 tumor slices and control OVA-Panc-02 tumor slices. In principal-component analysis, cholesterol was detected as a major component (Figure 5E). As measured by bulk tumor slices, the cholesterol content in the *Npc1l1*-KO/*Npc1l1*-overexpressing group showed a modest shift compared with its control group (Figures 5F and 5G). As expected, when clarifying the tumor cells by H&E staining (Figures S11B and S11C), the cholesterol content of tumor cells in the *Npc1l1*-KO group showed a significant decrease

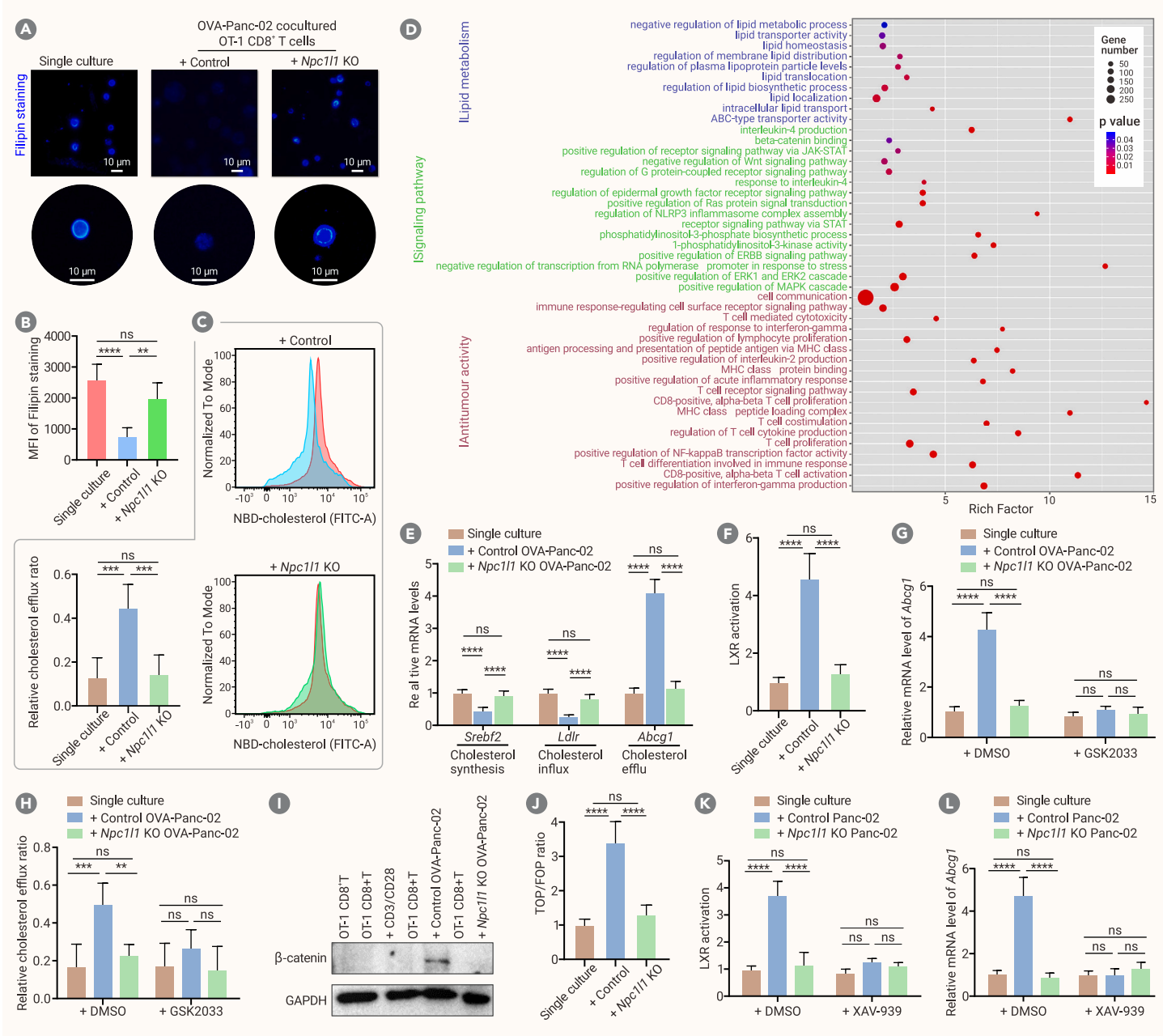

Figure 6. NPC1L1 on PAAD cells promotes the cholesterol efflux from anti-tumor CD8$^+$T cells (A and B) OT-I CTLs were single cultured or cocultured with *Npc1l1* KO/control OVA-Panc-02 cells for 7 h (0.1 μM filipin was added in medium). Representative images depicting the Filipin immunofluorescence in OT-I CTLs (A), and the mean fluorescence intensity was calculated by ImageJ software (B) (n = 5). (C) OT-I CTLs preloaded with NBD-cholesterol were cocultured with *Npc1l1* KO or control OVA-Panc-02 cells. The shift of mean fluorescence intensity of NBD immunofluorescence in OT-I CTLs depicting the cholesterol efflux (left), and the flow cytometric analysis of cholesterol efflux as shown (right) (n = 5). (D) Gene set enrichment analysis in the OT-I CTLs cocultured with control OVA-Panc-02 cells compared with the OT-I CTLs cocultured with *Npc1l1* KO OVA-Panc-02 cells. (E) Relative mRNA expression levels of the indicated cholesterol metabolism-related genes in single-cultured OT-I CTLs and OT-I CTLs cocultured with *Npc1l1* KO or control OVA-Panc-02 cells (n = 3). (F) LXR activity in single-cultured OT-I CTLs and in OT-I CTLs cocultured with control OVA-Panc-02 cells or *Npc1l1* KO OVA-Panc-02 cells is represented. OT-I CTLs were transfected with 200 ng of LXR reporter constructs together with 50 ng of pCMV-gal in the presence or absence of 20 ng of expression plasmids for LXR. Twenty-four hours after transfection, cells were cocultured with *Npc1l1* KO or control OVA-Panc-02 cells. After coculture for another 4 h, luciferase assays were performed (n = 5). (G) Relative mRNA expression levels of *Abcg1* in single-cultured OT-I CTLs and OT-I CTLs cocultured with OVA-Panc-02 cells in the absence or presence of LXR inhibitor GSK2033 (n = 5). (H) Mean fluorescence intensity of NBD-cholesterol efflux in single-cultured OT-I CTLs and OT-I CTLs cocultured with OVA-Panc-02 cells in the absence or presence of LXR inhibitor GSK2033. The ratio is that the fluorescence decreased part compared with the original intensity (n = 5). (I) Western blotting depicting the expression levels of β-catenin in OT-I CTLs cultured in the indicated conditions. (J) Top-flash (Wnt/β-catenin pathway-responsive firefly luciferase plasmid) reporter gene assay in single-cultured OT-I CTLs and OT-I CTLs cocultured with *Npc1l1* KO or control OVA-Panc-02 cells (n = 5). (K) LXR activity in single-cultured OT-I CTLs and OT-I CTLs cocultured with OVA-Panc-02 cells in the absence or presence of β-catenin inhibitor XAV-939 (n = 5). (L) Relative mRNA expression levels of *Abcg1* in single-cultured OT-I CTLs and OT-I CTLs cocultured with OVA-Panc-02 cells in the absence or presence of β-catenin inhibitor XAV-939 (n = 5). Error bars denote SEM. p values were calculated by two-way ANOVA with Tukey's multiple comparisons test in (E), (G), and (H, K, L). (B, C, F, and J) Analyzed by ordinary one-way variance (ANOVA) with Tukey's multiple comparisons test. $^{**}p < 0.01$, $^{***}p < 0.001$, $^{****}p < 0.0001$; ns, no significance.

relative to those in the control group (Figure 5H). To further determine the relative cholesterol content in CD8$^+$T cells in allografts, we stained CD8$^+$T cells in adjacent tumor slices by using an anti-CD8 antibody (Figure S11D). By merging the H&E staining and CD8 immunofluorescent staining, we delineated the corresponding regions of CD8$^+$T cells on tumor slices for cholesterol content analysis. Very impressively, as shown in Figure 5I, the cholesterol content of CD8$^+$T cells close to tumor cells in the *Npc1l1*-KO group showed a significant increase relative to those in the control group.

It has been reported that cholesterol content in the plasma membrane is critical for TCR activation of tumor-specific CD8$^+$T cells. Notably, by filipin staining, we found that cholesterol content, especially the cholesterol

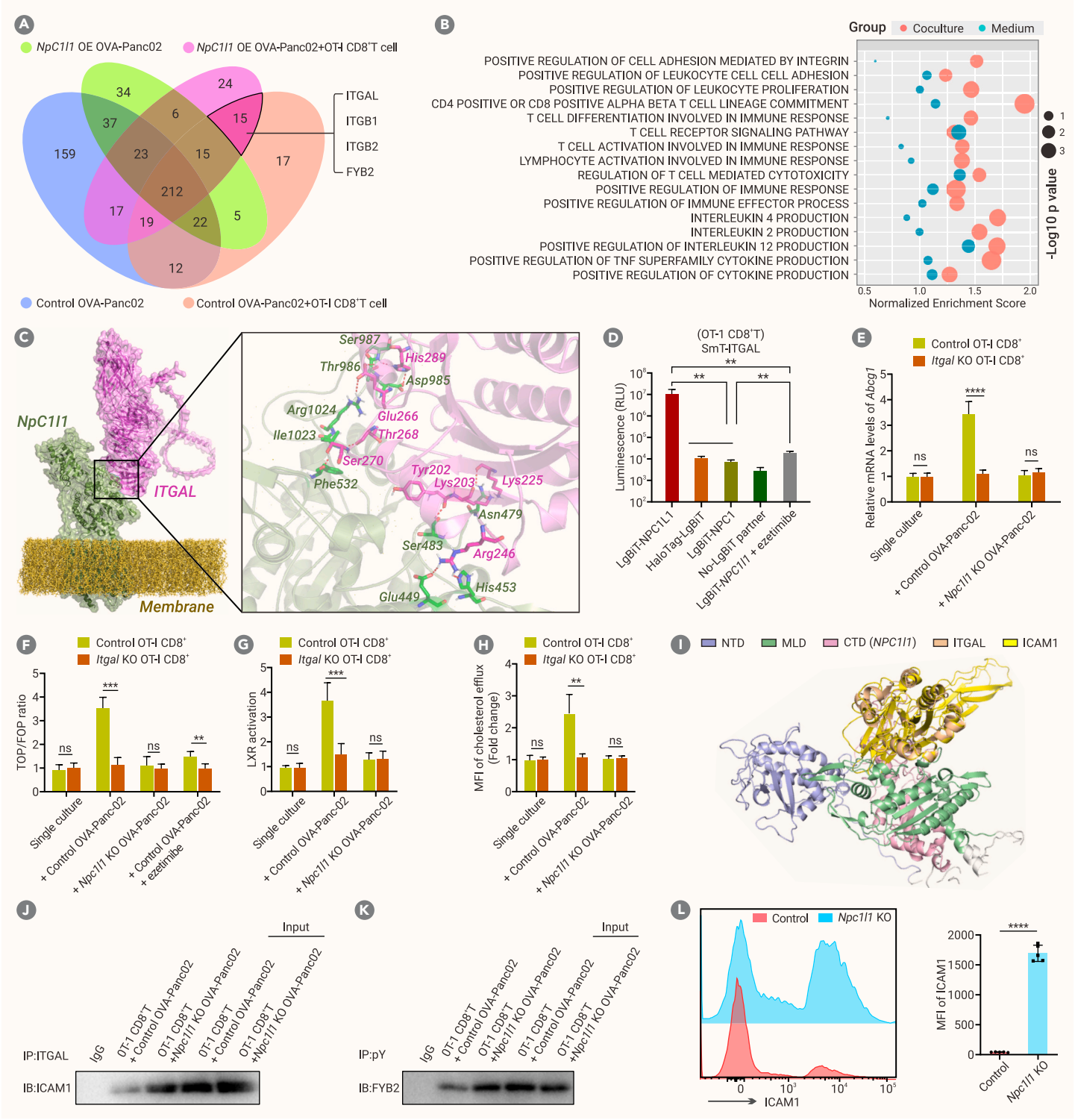

Figure 7. NPC1L1 functions as a checkpoint molecule on PAAD cells interacting with ITGAL on anti-tumor CD8$^+$T cells (A) OT-I CTLs were cocultured with control or Npc1l1-overexpressing OVA-Panc-02 cells, and coIP was performed using NPC1L1 antibody or Flag antibody to pull down the proteins that interacted with NPC1L1. LC-MS/MS was further performed to identify the interacting proteins. Venn diagram depicting overlap of interacting proteins. (B) Gene set enrichment analysis of T cell function signature in OT-I CTLs cocultured with control or *Npc1l1* KO OVA-Panc-02 cells, or treated with the supernatant of control or *Npc1l1* KO OVA-Panc-02 cells. OT-I CTLs were cocultured with control/*Npc1l1* KO OVA-Panc-02 cells or single cultured in the supernatant of control/*Npc1l1* KO OVA-Panc-02 cells for 4 h and rinsed off for RNA-seq. Colored bubbles represent the treatment condition. Red bubbles: OT-I CTLs cocultured with control/*Npc1l1* KO OVA-Panc-02 cells. Cyan bubbles: OT-I CTLs single cultured in supernatant of control/*Npc1l1* KO OVA-Panc-02 cells. GO analysis of differently expressed genes as shown. $\log_2$ fold change > 0, p_{adj} < 0.05. (C) Docking model depicting the interaction between the extracellular segment NPC1L1 (AF:Q9UHC9) and the extracellular segment of ITGAL (AF:P20701). (D) NanoBiT luciferase complementation assay in OT-I CTLs cocultured with OVA-Panc-02 cells. Cells were transfected with the denoted SmBiT and LgBiT constructs and assayed for luminescence 24 h later (n = 5). (E) LXR activity in single-cultured control/ITGAL KO OT-I CTLs or control/*Itgal* KO OT-I CTLs cocultured with control/*Npc1l1* KO OVA-Panc-02 cells (n = 5). (F) Top-flash (Wnt/β-catenin pathway-responsive firefly luciferase plasmid) reporter gene assay in single-cultured OT-I CTLs and OT-I CTLs cocultured with *Npc1l1* KO or control OVA-Panc-02 cells (n = 5). (G) Relative mRNA expression levels of *Abcg1* in single-cultured OT-I CTLs and OT-I CTLs cocultured with *Npc1l1* KO or control OVA-Panc-02 cells (n = 5). (H) MFI of cholesterol efflux in single-cultured OT-I CTLs and OT-I CTLs cocultured with *Npc1l1* KO or control OVA-Panc-02 cells (n = 5). (I) Docking model depicting NPC1L1 (PDB:6V3F) competitively binds to ITGAL (AF:P20701, alpha_L domain residue 153-334) against ICAM1 (PDB:1MQ8). (J) ITGAL immune complexes were immunoprecipitated from OT-I CTLs cocultured with *Npc1l1* KO or control OVA-Panc-02 cells and subjected to immunoblotting of ICAM1.

(legend continued on next page)

content in plasma membrane of OT-I CD8$^+$T cells cocultured with control OVA-Panc-02 cells, was significantly decreased in comparison with that in single-cultured OT-I CD8$^+$T cells, and this effect could be largely rescued when OT-I CD8$^+$T cells were cocultured with *Npc1l1*-KO OVA-Panc-02 cells (Figures 6A, 6B, and S12A). These phenomena strongly indicate that NPC1L1 may not only help PAAD cells to competitively uptake exogenous cholesterol against CD8$^+$T cells, but also provide PAAD cells with a chance to deprive the endogenous cholesterol from CD8$^+$T cells. To monitor the cholesterol flux of OT-I CD8$^+$T cells, we preloaded OT-I CD8$^+$T cells with 25-NBD cholesterol and cocultured these cells with *Npc1l1*-KO or control OVA-Panc-02 cells, respectively. Very impressively, under the monitoring of the living cell workstation, we found that control OVA-Panc-02 cells efficiently hijacked the intracellular NBD-cholesterol from OT-I CD8$^+$T cells they contacted (Video S9); in contrast, little hijack of NBD-cholesterol from OT-I CD8$^+$T cells was observed when OT-I CD8$^+$T cells were cocultured with *Npc1l1*-KO OVA-Panc-02 cells (Video S10). Expectedly, the same phenomena were observed from OVA-KPC cells (Videos S11 and S12). Correspondingly, a significantly increased cholesterol efflux was observed from OVA-Panc-02 cells cocultured OT-I CD8$^+$T cells relative to single-cultured OT-I CD8$^+$T cells, and this effect was abolished when OT-I CD8$^+$T cells were cultured with *Npc1l1*-KO OVA-Panc-02 cells (Figure 6C). These findings demonstrate that NPC1L1 not only allows PAAD cells to outcompete against CD8$^+$T cells in cholesterol uptake from the tumor microenvironment, but also hijack the intracellular cholesterol from anti-tumor CD8$^+$T cells via promoting their cholesterol efflux, thus leading to a complete cholesterol depletion from CD8$^+$T cells and therefore significantly suppressing their TCR activation and proliferation.

To further explore the underlying mechanism, we established four different culture systems for *Npc1l1*-KO or control OVA-Panc-02 cells and OT-I CD8$^+$T cells: (1) *Npc1l1*-KO or control OVA-Panc-02 cells were mix-cultured with OT-I CD8$^+$T cells, (2) *Npc1l1*-KO or control OVA-Panc-02 cells were cultured in the bottom, and OT-I CD8$^+$T cells were cultured in the upper, culture dish using a transwell chamber, (3) single-cultured OT-I CD8$^+$T cells were supplied with the culture supernatant of *Npc1l1*-KO or control OVA-Panc-02 cells, (4) single-cultured OT-I CD8$^+$T cells were supplied with normal culture medium with or without stimulation of α-CD3/CD28. Intriguingly, GO analyses of RNA-seq data showed that only under the coculture condition with control OVA-Panc-02 cells but not under the other culture condition, the cholesterol metabolism and anti-tumor activity of OT-I CD8$^+$T cells was significantly inhibited (Figure 6D), and these effects were abolished when OT-I CD8$^+$T cells were cocultured with Npc1l1-KO OVA-Panc-02 cells. We noticed that ABC-transporter activity was upregulated in OT-I CD8$^+$T cells cocultured with control OVA-Panc-02 cells relative to those cocultured with NPC1L1-KO OVA-Panc-02 cells (Figure 6D). Consistently, the mRNA expression levels of cholesterol efflux genes, *Abcg1*, were significantly increased, whereas cholesterol uptake gene, *Ldlr*, and cholesterol synthesis gene *Srebf2* were decreased in OT-I CD8$^+$T cells cocultured with control OVA-Panc-02 cells compared with those cocultured with *Npc1l1*-KO OVA-Panc-02 cells (Figure 6E). *In vivo*, CD8$^+$T cells sorted from subcutaneous transplantation tumors exhibit changes in cholesterol metabolism-related genes that are consistent with those observed *in vitro* (Figure S12B). In the cholesterol efflux assay, the relatively high intracellular cholesterol level in T cells can perform transcriptional factor and other functions, promoting the efflux of cholesterol from the cells. But our finding suggests that NPC1L1 may promote the efflux of intracellular cholesterol from anti-tumor CD8$^+$T cells and inhibit the cholesterol uptake and biogenesis of anti-tumor CD8$^+$T cells.

Liver X receptors (LXRs), belonging to the larger family of nuclear hormone receptors, play a critical role as cellular sensors of cholesterol balance. These transcription factors bind to specific DNA sequences and regulate gene expression in response to cholesterol levels. Under normal conditions, when intracellular cholesterol concentration increases, cells respond by producing oxysterols and activate the LXR signaling pathway to promote cholesterol efflux and inhibit cholesterol influx and synthesis. As shown in Figure 6F, the LXR activation was significantly increased in the OT-I CD8$^+$T cells cocultured with control OVA-Panc02 cells relative to that in single-cultured OT-I CD8$^+$T cells, and this effect was not observed when OT-I CD8$^+$T cells were cocultured with *Npc1l1*-KO OVA-Panc02 cells. Expectedly, the expression levels of *Abcg1* and cholesterol efflux of OT-I CD8$^+$T cells cocultured with control OVA-Panc02 cells were reversed in the presence of LXR inhibitor GSK2033 (Figures 6G and 6H). These findings demonstrated that the NPC1L1-induced cholesterol efflux from CD8$^+$T cells was mediated by LXR activation. We next sought to explore the mechanism by which NPC1L1 induces LXR activation. As shown in Figure 6D, accompanied with the shift of cholesterol metabolism and T cell activation, RNA-seq analyses also showed an upregulation of Wnt signaling pathway and β-catenin binding in OT-I CD8$^+$T cells mix-cultured with control OVA-Panc02 cells compared with those mix-cultured with *Npc1l1*-KO OVA-Panc02 cells. The Wnt/β-catenin signaling pathway is indeed a highly conserved regulatory cascade that plays a fundamental role in various biological processes, including the maintenance and regulation of hematopoietic stem cells, and has been implicated as a key regulator that can hinder the transition of CD8$^+$T cells from their precursor stages into mature, effector cells. Importantly, recent scientific findings have underscored the significant contribution of Wnt signaling to lipid homeostasis. The activation of the Frizzled/LRP (low-density lipoprotein receptor-related protein) receptor complex triggers a cascade of events that ultimately affects the activity of several transcription factors and nuclear receptors, which play a central role in governing lipid metabolism (PPARδ, RAR, LXR). As shown in Figures 6I and 6J, β-catenin expression level and activity were substantially increased in OT-I CD8$^+$T cells cocultured with control OVA-Panc02 cells relative to single-cultured OT-I CD8$^+$T cells, and were not activated in OT-I CD8$^+$T cells cocultured with *Npc1l1*-KO OVA-Panc02 cells. As expected, the LXR activation and the expression levels of *Abcg1* in OT-I CD8$^+$T cells cocultured with control OVA-Panc02 cells were dramatically reversed by Wnt/β-catenin signaling inhibitor XAV-939 (Figures 6K and 6L). Taken together, these findings demonstrated a critical role of β-catenin-LXR activation in mediating NPC1L1-induced *Abcg1* transcription and cholesterol efflux in anti-tumor CD8$^+$T cells.

NPC1L1 functions as a checkpoint molecule on PAAD cells to suppress tumor-specific CD8$^+$T cell activation via competitively interacting with ITGAL on CD8$^+$T cells against ICAM1 and further activate β-catenin-LXR signaling downstream of NPC1L1-ITGAL interaction to transactivate the cholesterol efflux genes

Since OT-I CD8$^+$T cells are supposed to efficiently kill murine cancer cells with OVA expression, we sought to elucidate why OT-I CD8$^+$T cells could not kill contacting OVA-Panc-02 cells efficiently but instead were hijacked with intracellular cholesterol during the life-and-death struggle. Immune checkpoint molecules on cancer cells, such as PD-L1, were known to function as brakes preventing tumor cells from being effectively killed by anti-tumor T cells. Since modest shift of PD-L1 expression levels were observed between Npc1l1 KO and control Panc-02 cells, and NPC1L1 is a transmembrane protein, we hypothesized that NPC1L1 may function as a checkpoint-like molecule on PAAD cells to efficiently suppress the cytotoxicity of anti-tumor CD8$^+$T cells and further provide PAAD a chance to hijack the cholesterol from CD8$^+$T cells. To probe the potential interaction partner of NPC1L1 on anti-tumor CD8$^+$T cells, we transfected OVA-Panc-02 cells with a Flag-labelled *Npc1l1*-overexpressing plasmids, and cocultured *Npc1l1*-overexpressing OVA-Panc-02 cells or control OVA-Panc-02 cells with OT-I CD8$^+$T cells for 5 h, and then immunoprecipitated the protein from the coculture system or from the single-culture system with anti-Flag or anti-NPC1L1 antibody. By mass spectrometry, we compared the NPC1L1 interacting proteins between the coculture system and the single-culture system, and found that ITGAL, ITGB1, ITGB2, and FYB2, were pulled down by both Flag antibody and NPC1L1 antibody in the coculture groups but not in the single-culture groups (Figure 7A). ITGAL is specifically expressed on leukocytes, and ITGAL/ITGB2 is a receptor for ICAM on antigen-presenting cells (APCs) and functions as a costimulatory signal molecule responsible for several T cell functions, including APC conjugate stabilization to T cell, activation and killing target cells.[59–61] Upon TCR stimulation by encountering APCs, T cells experience a dramatic increase in their ability to adhere to these APCs through integrins and receive antigen-specific signals for

(K) IP was performed using a mixture of anti-phosphotyrosine (pY) Abs (4G10 and p-Tyr100) and analyzed by IB to visualize FYB2. (L) Representative FACS graphs (left) and statistical analysis (right) of mean fluorescence intensity of ICAM1 immunofluorescence in *Npc1l1* KO and control OVA-Panc-02 cells (n = 5). Error bars denote SEM. p values were calculated by unpaired two-tailed t test in (B) and (L). Statistical significance was assessed by two-way ANOVA with Tukey's multiple comparisons test in (E)–(H). (D) Analyzed by ordinary one-way variance (ANOVA) with Tukey's multiple comparisons test. $^{**}p < 0.01$, $^{***}p < 0.001$, $^{****}p < 0.0001$; ns, no significance.

executing a range of immune responses tailored to the threat encountered. Meanwhile, FYB2 was a critical adaptor protein to couple TCR activation to increase in integrin avidity.[62] Consistently, the results from RNA-seq showed that the pathway of positive regulation of leukocyte adhesion mediated by integrin, leukocyte proliferation, and cytotoxicity were enriched in OT-I CD8$^+$T cells cocultured with Npc1l1 KO OVA-Panc-02 cells relative to those cocultured with control Panc-02 cells (Figure 7B).

Based on our docked result, among ITGAL/ITGB1/ITGB2, the extracellular region of ITGAL showed the highest affinity score with the extracellular region of NPC1L1, and the average affinity score of the top 5 binding sites was 1,637.15. The αI domain of ITGAL interacts with the MLD and CTD domain of NPC1L1 (Figure 7C). To further determine the interaction between PAAD cell-expressed NPC1L1 and CD8$^+$T cell-expressed ITGAL, we established a NanoBiT Protein:Protein Interaction System. NanoLuc Binary Technology (NanoBiT) is a cutting-edge bioluminescent assay designed for the real-time monitoring and quantification of protein-protein interactions (PPIs) in living cells. Small BiT (SmBiT; 11 amino acids) was fused to Itgal and a large BiT (LgBiT; 17.6 kDa) subunit was fused to Npc1l1 and, when expressed, the PPI brings the subunits to assemble to reconstitute a functional NanoLuc luciferase enzyme that results in a luminescent signal (Figure S12D). In our experiments, we transfected OVA-Panc-02 cells with LgBiT-Npc1l1 and OT-I CD8$^+$T cells with SmBiT-Itgal, under the conditions of coculture, the luminescence generated from the interaction between OVA-Panc-02 cells expressing LgBiT-Npc1l1 and OT-I CD8$^+$T cells expressing SmBiT-Itgal is 1,000-fold higher than the SmBiT fusion coexpressed with LgBiT-Npc1, HaloTag-LgBiT, the NanoBiT negative control, indicating a specific PPI between OVA-Panc-02-expressed NPC1L1 and OT-I CD8$^+$T cell-expressed ITGAL (Figure 7D). Notably, we found that NPC1L1 expressed on OVA-Panc-02 cells only interacts with ITGAL expressed on OT-I CD8$^+$T cells but not that on wild-type CD8$^+$T cells (Figure S12C) or that on other OVA-Panc-02 cells (Figure S12E). Intriguingly, NPC1L1 expressed on OVA-Panc-02 cells also showed an affinity to ITGAL on NK and macrophagy (Figures S12F and S12G), suggesting that the interaction between PAAD cell-expressed NPC1L1 and immunocyte-expressed ITGAL may be dependent of specific recognition between cancer cell and immunocytes, such as MHC. At the same time, ezetimibe can significantly disrupt the binding between OVA-Panc-02 cell expression and OT-I CD8$^+$T cells (Figure 7D).

It is known that Wnt/β-catenin and integrin are orchestrated in regulating various signaling cascades. To further determine whether ITGAL is involved in NPC1L1-induced β-catenin-LXR activation and cholesterol efflux, we established ROSA26_Cas9$^{[CKI/CKI]}$ OT-1 mice and silenced *Itgal* by sgRNA in isolated OT-I CD8$^+$T cells. As shown in Figures 7E–7G, when cocultured with control OVA-Panc-02 cells, the activation of β-catenin and LXR, and the subsequent transactivation of *Abcg1*, were significantly decreased in *Itgal* KO OT-I CD8$^+$T cells relative to that in control OT-I CD8$^+$T cells and close to the level of single-cultured OT-I CD8$^+$T cells. Correspondingly, the cholesterol efflux from *Itgal* KO OT-I CD8$^+$T cells was efficiently prevented compared with control OT-I CD8$^+$T cells when cocultured with OVA-Panc-02 cells. Meanwhile, we also noticed that, when cocultured with *Npc1l1* KO OVA-Panc-02 cells, little shift of β-catenin-LXR signaling and cholesterol efflux was observed between *Itgal* KO and control OT-I CD8$^+$T cells (Figure 7H), indicating NPC1L1 as an exclusive protein on PAAD cells to induce the cholesterol efflux from anti-tumor CD8$^+$T cells.

It has been known that CD28 and CTLA-4 on T cells share B7 family ligands B7-1 (CD80) and B7-2 (CD86) on APCs, and the affinity of CTLA-4 is 20–100 times higher than that of CD28. As an inhibitory receptor for B7, CTLA-4 functions as a counterpart to CD28 for CD80/CD86, thereby transmitting inhibitory signals into the T cell, effectively dampening the immune response. Since the ITGAL/ITGB2 is a receptor for ICAM on APCs and functions as a costimulatory signal molecule responsible for T cell full activation, we deduced that NPC1L1 on PAAD cells may function as an inhibitory ligand for ITGAL and competitively interact with ITGAL against ICAM1 to suppress T cell activation and cytotoxic killing. We also docked ICAM1 onto the αI domain of ITGAL and noticed significant clashing with the NPC1L1 after alignment of the ITGAL structure, suggesting that NPC1L1 competes with ICAM1 during binding to ITGAL (Figure 7I). Co-immunoprecipitation assay further showed that the interaction between ITGAL and ICAM-1 was substantially increased in the protein lysis from cocultured OT-I CD8$^+$T cells and *Npc1l1* KO OVA-Panc-02 cells relative to that in the protein lysis from cocultured OT-I CD8$^+$T cells and control OVA-Panc-02 cells (Figure 7J). FYB2 has been identified as an adaptor phosphoprotein required for the TCR signaling pathway and integrin-mediated adhesion. As shown in Figure 7A, FYB2 was also immunoprecipitated in the NPC1L1-ITGAL complex. We then further immunoprecipitated the protein lyses from OT-I CD8$^+$T cells cocultured with *Npc1l1* KO or control OVA-Panc-02 cells using anti-phosphotyrosine antibodies followed by western blotting with anti-FYB2 antibody. Expectedly, tyrosine phosphorylation of FYB2 increased in OT-I CD8$^+$T cells cocultured with *Npc1l1* KO OVA-Panc-02 cells relative to those cocultured with control OVA-Panc-02 cells (Figure 7K). This evidence strongly suggests that NPC1L1 functions as an inhibitory ligand for ITGAL and competitively binds to ITGAL against ICAMs to efficiently suppress the activation and cytotoxicity of anti-tumor CD8$^+$T cells and provide PAAD cells a chance to hijack the intracellular cholesterol from contacting CD8$^+$T cells instead. More importantly, we found that the expression levels of ICAM on *Npc1l1* KO OVA-Panc-02 cells were significantly increased relative to those on control OVA-Panc-02 cells (Figure 7L), which further explains why NPC1L1 efficiently suppressed the activation of ITGAL by ICAM1.

Collectively, our findings indicate that PAAD utilizes their expressed NPC1L1 protein as a checkpoint to dampen the cytotoxicity of anti-tumor CD8$^+$T cells by downregulating ICAM1 expression levels and competitively interacting with ITGAL on contacting tumor-specific CD8$^+$T cells against ICAM1. Moreover, NPC1L1-ITGAL interaction activates β-catenin-LXR signaling and boosts intracellular cholesterol efflux from anti-tumor CD8$^+$T cells, thus providing PAAD cells a chance to hijack the intracellular cholesterol from the contacting anti-tumor CD8$^+$T cells, ultimately leading to substantial suppression of the CD8$^+$T cells' ability to eliminate cancer cells.

The NPC1L1 blockade ezetimibe facilitates the anti-tumor response mediated by CD8$^+$T cells and synergizes with PD-1 inhibitor to improve its therapeutic efficacy in PAAD

Based on the crucial role of NPC1L1 in suppressing the anti-tumor activity of CD8$^+$T cells in PAAD, we examined the promise of NPC1L1 as a target to improve the anti-tumor immunity in PAAD. Ezetimibe is a pharmaceutical agent recognized for its selective and potent inhibitory action on NPC1L1 with a favorable safety profile that has been prescribed for patients suffering from hypercholesterolaemia.[63] In a subcutaneous allograft model (Figure S13A), although anti-PD-1 monotherapy showed little inhibition of tumor growth of Panc-02 cell-derived allografts, ezetimibe monotherapy, especially high-dose ezetimibe (30 mg/kg/day) showed better inhibitory efficacy than PD-1 monotherapy. Impressively, high-dose ezetimibe showed a synergistic effect with the anti-PD-1 antibody and efficiently suppressed the growth of the allografts (Figures 8A and 8B). In an intraperitoneal allograft model, the combo therapy of high-dose ezetimibe plus PD-1 antibody also significantly inhibited the implantation and invasion of PAAD cells in the peritoneal cavity characterized by substantially reduced tumor burden and ascites (Figures 8C and S13B). Correspondingly, although PD-1 monotherapy showed little effect on CD8$^+$T cell infiltration, the combo therapy of ezetimibe plus PD-1 antibody significantly increased the number of CD8$^+$T cells in allografts (Figures 8D and S13D), and showed potentiation of proliferation, activation, and cytotoxicity in CD44$^+$CD8$^+$T cells (Figure S13E) with little effect on peripheral blood (Figure S14A). To further validate the efficacy of combining PD-1 antibody and ezetimibe in primary PAAD, we conducted additional experiments in a KPC mouse model (Figure S13C). As shown in Figures 8E–8G, PD-1 antibody monotherapy and ezetimibe treatment exhibited a certain degree of therapeutic effect, and ezetimibe synergistically improved the efficacy of PD-1 antibody. As expected, although ezetimibe less than 50 μM showed modest inhibition on the proliferation of human and mouse PAAD cell lines *in vitro* (Figures S14B–S14D), it significantly decreased the cholesterol uptake of the OVA-Panc-02 cells (Figure S14E) and substantially promoted the cholesterol uptake of the cocultured OT-I CD8$^+$T cells (Figure S15A). Meanwhile, the β-catenin/LXR activation, *Abcg1* transcription and cholesterol efflux of the OT-I CD8$^+$T cells cocultured with OVA-Panc-02 cells were significantly inhibited by ezetimibe (Figures S15B and S15C). Intriguingly, although ezetimibe does not interact with NPC1L1 on the docked interface between NPC1L1 and ITGAL, in the conformation induced by ezetimibe binding, NPC1L1 has a higher docking score (weaker binding) with ITGAL, compared with NPC1L1 in the conformation without ezetimibe binding (Figure 8H).

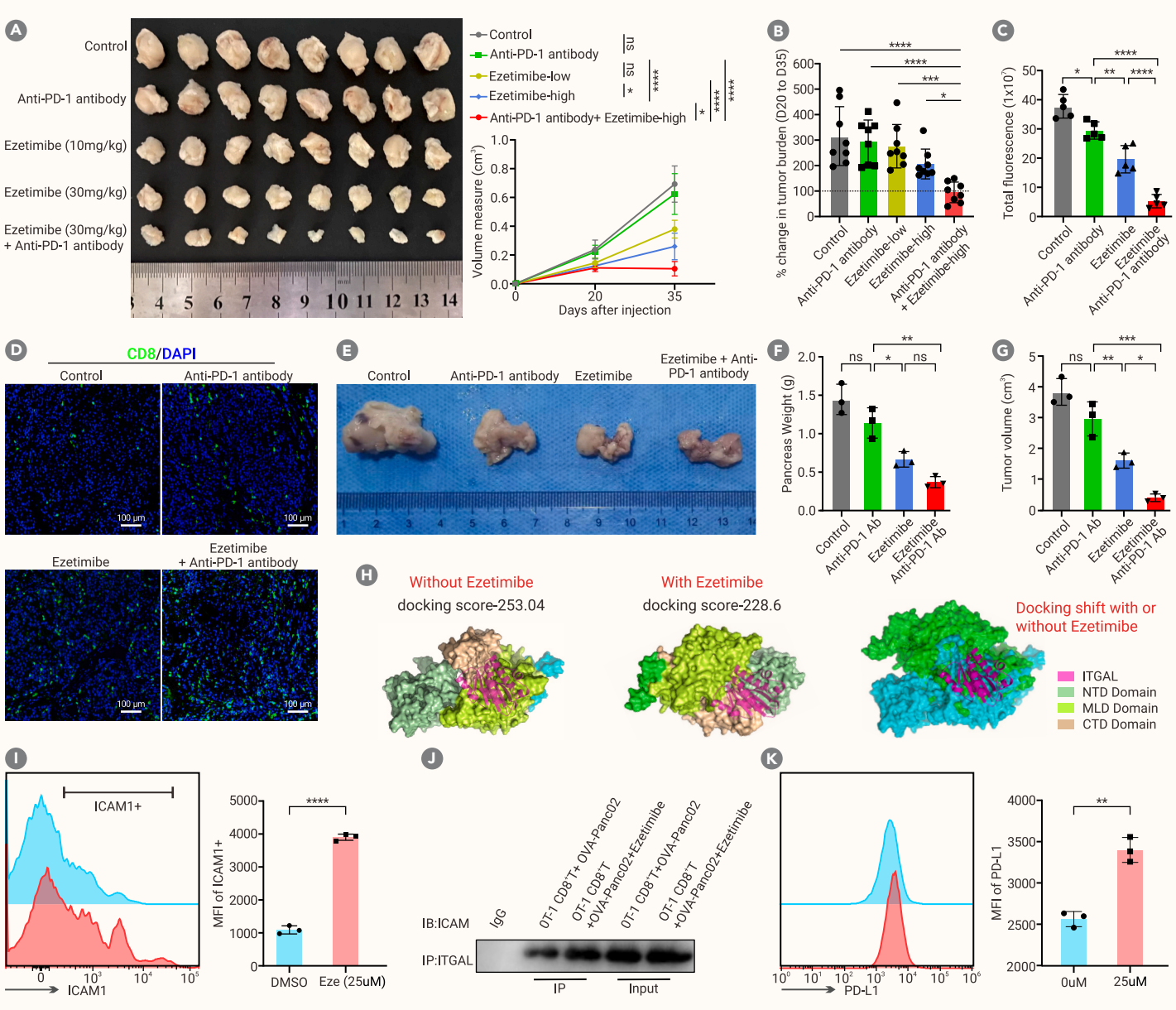

Figure 8. NPC1L1 inhibitor ezetimibe sensitizes PAAD tumors to PD1 antibody therapy (A and B) C57BL/6 mice were inoculated subcutaneously with 1 × 10^6 Panc-02 cells, and were treated with either vehicle alone (PBS) or PD1 antibody (10 mg/kg, once/3 days), low-dose ezetimibe (10 mg/kg, once/day), high dose ezetimibe (30 mg/kg, once/day), PD1 antibody (10 mg/kg, once/3 days) + ezetimibe (30 mg/kg, once/day) 5 days after inoculation. Tumors were dissected and dissociated at day 35 after the treatments for analysis. (A) Representative gross appearance of the subcutaneous allografts in the indicated groups. (B) Statistical analysis of tumor size in the indicated groups (n = 8). (C) C57BL/6 mice were inoculated intraperitoneally with 1 × 10^6 Panc-02-luc cells, and were treated with either vehicle alone (PBS) or PD1 antibody (10 mg/kg, once/3 days), ezetimibe (30 mg/kg, once/day), PD1 antibody (10 mg/kg, once/3 days) + ezetimibe (30 mg/kg, once/day) 5 days after inoculation. Tumor growth was monitored through the IVIS bioluminescent imaging system. (D) Representative immunofluorescent staining of tumor-infiltrated $CD8^+$T cells in the indicated groups. (E–G) KPC mice were treated with either isotype antibody or PD1 antibody (10 mg/kg, once/3 days), ezetimibe (30 mg/kg, once/day), PD1 antibody (10 mg/kg, once/3 days) + ezetimibe (30 mg/kg/day) from 15 weeks old. At age 22 weeks, the mouse was sacrificed and dissected to obtain the pancreatic tumor for analysis and photography. (E) Representative gross appearance of the pancreases with tumors in the indicated groups. (F and G) Statistical analysis of pancreas weight and tumor size in the indicated groups (n = 3). (H) Docking model depicting the interaction between Panc-02-expressed NPC1L1 and $CD8^+$T cell-expressed ITGAL (AF:P20701, alpha_L domain residue 153-334) with (PDB:6V3H) or without (PDB:6V3F) ezetimibe binding to NPC1L1. (I) Representative FACS graphs (left) and statistical analysis (right) of mean fluorescence intensity of ICAM1 immunofluorescence in Panc-02 cells with or without ezetimibe treatment (n = 3). (J) ITGAL immune complexes were immunoprecipitated from OT-I CTLs cocultured with OVA-Panc-02 cells with or without ezetimibe treatment and subjected to immunoblotting of ICAM1. (K) Representative FACS graphs (left) and statistical analysis (right) of mean fluorescence intensity of PD-L1 immunofluorescence in Panc-02 cells at different time points after ezetimibe treatment (n = 3). Error bars denote SEM. p values were calculated by unpaired two-tailed t test in (I) and (K). Statistical significance was assessed by two-way ANOVA with Tukey's multiple comparisons test in (A, right). (B, C, F, and G) Analyzed by ordinary one-way variance (ANOVA) with Tukey's multiple comparisons test. *p < 0.05, **p < 0.01, ***p < 0.001, ****p < 0.0001; ns, no significance.

Notably, although $CD8^+$T cells expressed little expression levels of *Npc1l1* (Figures S3, S15D, and S15E), we did observe that ezetimibe significantly increased the activation, proliferation, and cytotoxicity of single-cultured $CD8^+$T cells *in vitro* in the presence of α-CD3/CD28 (Figure S16). It has been reported that ezetimibe stimulates fatty acid oxidation by increasing the level of carnitine palmitoyltransferase 1A in $CD8^+$T cells, which is associated to $CD8^+$ central memory T cells and the mTOR pathway.[64] Our RNA-seq analyses showed that ezetimibe stimulated the PI3K signaling pathway and IL-23 production in $CD8^+$T cells in the presence of α-CD3/CD28 (Figure S15F). We also performed additional *in vitro* experiments utilizing KPC cells to demonstrate that ezetimibe effectively liberated $CD8^+$T cells and restored their anti-tumor activity, which would otherwise have been suppressed by PAAD cells via NPC1L1 (Figure S15G). Expectedly, similar to *Npc1l1* silencing, ezetimibe treatment also increased ICAM-I on Panc-02 cells (Figure 8I) and promoted the interaction between OVA-Panc02-expressed ICAM1 and OT-I $CD8^+$T cell-expressed ITGAL (Figure 8J), while intriguingly we found that ezetimibe treatment increased the protein levels

of PD-L1 on Panc-02 cells (Figure 8K), which is contract to *Npc1l1* silencing but well explained why ezetimibe synergized with anti-PD-1 treatment. Since ezetimibe does not interact with NPC1L1 on the docked interface between NPC1L1 and ITGAL, further study should be conducted to investigate how ezetimibe can inhibit the interaction between NPC1L1 and ITGAL. Meanwhile, the upregulation of ICAM/PD-L1 on PAAD cells in the presence of ezetimibe should be further elucidated. Taken together, this evidence suggests that ezetimibe combo therapy might be a desirable strategy to augment the efficacy of PD-1 blockade in PAAD.

DISCUSSION

Although the views on the origin of cancer as a metabolic disease have been under debate during recent decades since the proposition of the Warburg effect, it is well accepted that metabolic reprogramming is a hallmark of cancers critically attributable to the malignant behaviors of cancer cells,[17,18] but why the metabolic characteristics varied across different cancer types and how cancer cells initiate a unique metabolic reprogramming to meet the requirements of fast growth and immune escape remains largely elusive. Cholesterol is the main membrane lipid necessary for cancer cells to grow rapidly. The *de novo* cholesterol synthesis needs oxygen for the enzyme reaction of squalene monooxygenase.[28] Since an anoxic microenvironment is an important feature of many solid tumors, such as PAAD,[2] how these cancer cells evolutionarily adapt to the crisis of insufficient endogenous cholesterol synthesis is quite an interesting question to be elucidated.

In this study, we showed that PAAD cells ingeniously overcome the cholesterol shortage and immune surveillance via ectopically overexpressing NPC1L1. NPC1L1 is a cholesterol transporter normally expressed in intestine and liver for the absorption of cholesterol with little expression in the pancreas. We for the first time revealed that NPC1L1 on PAAD cells functions as a two-pronged checkpoint not only directly suppressing the TCR activation but also hijacking the intracellular cholesterol from anti-tumor CD8$^+$T cells to exhaust their cholesterol possession, which is essential for their anti-tumor activity and proliferation.

During the process of carcinogenesis, somatic mutations occur in oncogenes and tumor suppressor genes within cells. These alterations lead to widespread changes in gene expression profiles, ultimately triggering metabolic reprogramming that facilitates the transformation of cells into cancerous ones.[65,66] NPC1L1 is normally highly expressed in liver and small intestine with undetectable expression levels in pancreas. We found that the highly increased mRNA level of *NPC1L1* in PAADs was associated with a demethylated DNA status. The mRNA levels of *NPC1L1* were positively correlated with those of the demethylase TET3. In addition, the mRNA expression levels of TET3 were increased in PAAD tissue relative to normal pancreatic tissue. Furthermore, we found that the expression levels of TET3 were higher in Kras mutant PAAD than in Kras wild-type PAAD. NPC1L1 overexpression may be a consequence of Kras-induced TET3 activation, but the precise mechanism underlying the highly increased expression level of NPC1L1 in PAAD is worthy of further exploration.

Of note, besides NPC1L1, PAAD cells also express another cholesterol transporter, LDLR. Why do PAAD cells express both NPC1L1 and LDLR? We found that *Npc1l1* KO decreased but did not completely abolish the cholesterol uptake of PAAD cells. Meanwhile, *Npc1l1* KO significantly reversed the anti-tumor activity of tumor-specific CD8$^+$T cells. NPC1L1 shares approximately 50% amino acid similarity with NPC1, a protein that plays a crucial role in the intracellular trafficking of cholesterol. Unlike NPC1, which is located in the cytoplasm, NPC1L1 is a transmembrane protein.[6] Very importantly, our study for the first time revealed NPC1L1 as a checkpoint-like molecule on PAAD cells efficiently suppressing the TCR activation and cytotoxicity of anti-tumor CD8$^+$T cells, highlighting a more important non-canonical function of NPC1L1 in charging the anti-tumor activity rather than as a cholesterol transporter in PAADs.

Integrins play important roles in T cell activation and cytotoxicity. ITGAL is an important costimulatory molecule on CD8$^+$T cells critically attributable for the adhesion of CD8$^+$T cell to target cell for lysis when it interacts with and is activated by its activating partner ICAM-1 on tumor cells.[59–61] We demonstrated that NPC1L1 suppresses the expression levels of ICAM-1 on PAAD cells, and further competitively interact with ITGAL on anti-tumor CD8$^+$T cells against ICAM-1-ITGAL interaction. By this means, NPC1L1 substantially inhibits the TCR activation and cytotoxicity of CD8$^+$T cells, preventing PAAD cells from being efficiently killed by anti-tumor CD8$^+$T cells. CTLA-4 stands as the initial immune checkpoint receptor subjected to clinical targeting, and it is uniquely expressed on T cells, where it predominantly governs the intensity of the initial phases of T cell activation. CD28 and CTLA-4 share identical ligands — CD80 and CD86.[67] Whereas the interaction between CD28 and B7-1/2 ligands provides a costimulatory signal that encourages T cell proliferation and activation, the engagement of CTLA-4 with B7-1/2 serves as a counterbalancing coinhibitory signal, which dampens the early stages of T cell activation.[68] Given that CTLA-4 exhibits a significantly greater binding affinity for both B7-1 (CD80) and B7-2 (CD86) ligands compared with CD28, its presence on the T cell surface effectively diminishes T cell activation by competitively displacing CD28 in binding these ligands. Furthermore, CTLA-4 actively transmits suppressive signals into the T cell, thereby attenuating the immune response.[68] Similar to CTLA-4, we showed that NPC1L1 is an essential "brake" on PAAD cells to restrain the activation of ITGAL on CD8$^+$T cells, supporting evidence that NPC1L1 is an endogenous antagonist for ITGAL to inhibit "outside-in" signaling and thus suppress the anti-tumor activity of CD8$^+$T cells. CD28's influence on T cell activation is contingent upon prior engagement of TCR by its specific antigen. We speculate that NPC1L1-ITGAL interaction between PAAD cell and CD8$^+$T cell may also be dependent of antigen recognition. FYB2 has been discovered as a new adapter protein essential for TCR signaling and integrin-dependent adhesion. Studies have shown that FYB2 assumes a distinctive function in T cells by participating in both the immediate TCR signaling cascade and the inside-out signaling pathways. These pathways culminate in the activation of integrins and subsequent adhesion of T cells, which are indispensable steps for the successful activation and cytotoxic capabilities of CD8$^+$T cells. As shown in Figure 7A, FYB2 was also pulled down by NPC1L1 immunoprecipitation, further supporting a critical role of NPC1L1 involved in regulating integrin-mediated TCR activation. The precise signaling pathway by which NPC1L1-ITGAL blocks T cell activation remains to be investigated. Intriguingly, we found that PAAD cell-expressed NPC1L1 can suppress the expression levels of ICAM1 and sustain the expression levels of PD-L1. These effects may also be attributable to the suppression of TCR activation of CD8$^+$T cells, and the underlying mechanism should be further elucidated. In addition, T cell immunity and innate immunity are delicate and regulated by the Hippo signaling pathway,[69] the potential exists for NPC1L1 to influence T cell activation through the Hippo signaling pathway. Intriguingly, as shown in Figure S12, PAAD cell-expressed NPC1L1 can also interact with ITGAL expressed on NK and macrophage but cannot interact with ITGAL enforced on non-anti-tumor CD8$^+$T cells or PAAD cells. It is reported that ITGAL is involved in NK cytotoxicity and macrophage phagocytosis.[70,71] Meanwhile, as shown in Figure 2A, besides CD8$^+$T cells, the frequencies of macrophages also increased in *Npc1l1*-KO tumors relative to those in control tumors, and our flow cytometric analysis demonstrated that the priming of CD8$^+$T cells was also modestly increased in the *Npc1l1*-KO group relative to the control group (Figures 2I and 2L). We cannot exclude that NPC1L1 may also affect the anti-tumor activity of NK/macrophages besides suppressing CD8$^+$T cells, and the potential role of NPC1L1 in regulating the activity of macrophage and NK cells should be explored in future studies.

Of note, we found that NPC1L1-ITGAL interaction can further activate LXR-mediated transcriptions of *Abcg1* to promote the efflux of plasma membrane cholesterol from anti-tumor CD8$^+$T, providing PAAD cells a chance to acquire intracellular cholesterol from anti-tumor CD8$^+$T cells, and leading to an exhaustion of cholesterol in CD8$^+$T cells. Since the content of free cholesterol in plasma membrane is critical for TCR activation and proliferation of CD8$^+$T cells,[36] by hijacking the intracellular cholesterol from CD8$^+$T cells, NPC1L1 can further help PAAD cells to suppress the activation and proliferation of anti-tumor CD8$^+$T cells, eventually resulting in severe inhibition of the anti-tumor activity of CD8$^+$T cells. NPC1L1 firstly functions as a checkpoint preventing PAAD cells from being killed by anti-tumor CD8$^+$T cells, and further functions as a "pump" draining the cholesterol out of contacting CD8$^+$T cells. This two-step function may explain why NPC1L1 plays a critical role in suppressing the anti-tumor activity of CD8$^+$T cells in PAADs. Meanwhile, besides the upregulations of *Abcg1*, the cholesterol uptake and biosynthesis genes, *Ldlr* and *Srebp2*, were decreased in OT-I CD8$^+$T cells co-cultured with NPC1L1-proficient OVA-Panc-02 cells, and this effect was abolished when OT-I CD8$^+$T cells were cocultured with *Npc1l1*-KO Panc-02 cells, indicating that NPC1L1 may also inhibit the cholesterol uptake and synthesis of CD8$^+$T cells to block their cholesterol acquisition, thus resulting in a complete cholesterol depletion of CD8$^+$T cells. Our study provides evidence that NPC1L1 is critical for PAAD cells to reprogram the cholesterol metabolism between cancer cells and CD8$^+$T cells in the tumor microenvironment to suppress the

anti-tumor activity. The molecular mechanism responsible for NPC1L1-induced cholesterol reprogramming in $CD8^+$T should be further explored. Since the NPC1L1 localizes on the lipid raft membrane domain, lipid rafts may play an important role in the direct interaction between NPC1L1 and T cells, which is worthy of further study.

Numerous research studies have consistently demonstrated that suppressing cholesterol synthesis has adverse effects on cancer cells.[72] Indeed, statins, a group of drugs that work by inhibiting HMG-CoA reductase—the key regulatory enzyme in cholesterol biosynthesis—have been investigated as potential anti-cancer agents in numerous clinical trials. While these drugs effectively curb cholesterol production, it is worth noting that the cholesterol synthesis pathway is integral to normal cellular functioning. Thus, inhibition of cholesterol synthesis can inadvertently compromise the structural integrity and functionality of cellular membranes, potentially by impacting membrane fluidity or hindering the formation of lipid rafts.[73] This strategy thus has only a limited influence on cell fate, particularly in tumors.[74] On the contrary, while cholesterol synthesis has garnered significant attention in cancer research, the role of cholesterol uptake pathways has been relatively understudied. However, our findings demonstrate that cholesterol uptake pathways indeed play a pivotal role in the development and progression of PAAD. We, for the first time, showed here that ezetimibe, a commonly used drug approved for the clinical treatment of hypercholesterolemia, efficiently rescued the anti-tumor immune function of $CD8^+$ in PAAD and synergized to anti-PD-1 antibody therapy. Intriguingly, although the binding site of ezetimibe on NPC1L1 is not located in the interface between NPC1L1 and ITGAL, we do observe an interruption of NPC1L1-ITGAL under the presence of ezetimibe, which may be explained by allosteric effect. Since ezetimibe could offer an additional benefit by improving the therapeutic efficacy of anti-PD-1 therapy in PAAD, iterative small molecules that can specifically target the interface between NPC1L1-ITGAL may provide more promising effect on normalizing the anti-tumor immunity of $CD8^+$T cells in PAADs and sensitizing PAADs to immunotherapy. The current evidence suggests that monotherapy with checkpoint inhibitors is not a promising strategy for the general population of patients with PAAD. However, combination treatment with checkpoint blockade and NPC1L1 targeting may induce a significant clinical response in the subset of NPC1L1high PAAD patients, which accounts for as many as 16% of PAAD patients (Figure 1D). Meanwhile, it should be considered that the anti-tumor efficacy of ezetimibe or other cholesterol-lowering treatments in mouse models applied substantially higher doses (e.g., 60 mg simvastatin per kg per day),[75] further work still needs to be performed to realize this potential in clinic. At least, this study presents a new concept for improving the anti-tumor activity and immunotherapy efficacy in PAADs by targeting NPC1L1-mediated TCR inactivation and cholesterol deprivation.

CONCLUSION

This study is the first to establish a critical role of NPC1L1 as a two-pronged checkpoint suppressing the cytotoxicity of anti-tumor $CD8^+$T cells and hijacking the intracellular cholesterol from anti-tumor $CD8^+$T cells. Our findings well explained how PAAD cells evolutionarily reprogram their cholesterol metabolism to confronting the adversity of *de novo* cholesterol synthesis in hypoxic challenge and escaping the immune surveillance, suggesting that unique metabolic characteristics of different cancers may be adaptive choices for varied survival pressures. The immunosuppressive tumor microenvironment renders PAAD highly malignant and largely refractory to immunotherapy, which is a big obstacle in the clinic. Our study reveals NPC1L1 as a metabolic vulnerability target to improve the anti-tumor activity of PAAD, strongly suggesting NPC1L1 inhibition as a promising strategy for sensitizing PAAD to immunotherapy.

DATA AND CODE AVAILABILITY

Data are available from the corresponding author upon reasonable request. The raw bulk RNA-seq data detailed in this publication are deposited in the SRA (Sequence Read Archive) with the accession number PRJNA1210808.

REFERENCES

1. Fridman, W.H., Pagès, F., Sautès-Fridman, C. et al. (2012). The immune contexture in human tumours: impact on clinical outcome. *Nat. Rev. Cancer* **12**:298–306.
2. Joyce, J.A. and Fearon, D.T. (2015). T cell exclusion, immune privilege, and the tumor microenvironment. *Science* **348**:74–80.
3. Tumeh, P.C., Harview, C.L., Yearley, J.H. et al. (2014). PD-1 blockade induces responses by inhibiting adaptive immune resistance. *Nature* **515**:568–571.
4. Pardoll, D.M. (2012). The blockade of immune checkpoints in cancer immunotherapy. *Nat. Rev. Cancer* **12**:252–264.
5. Mellman, I., Coukos, G. and Dranoff, G. (2011). Cancer immunotherapy comes of age. *Nature* **480**:480–489.
6. Brahmer, J.R., Tykodi, S.S., Chow, L.Q.M. et al. (2012). Safety and activity of anti-PD-L1 antibody in patients with advanced cancer. *N. Engl. J. Med.* **366**:2455–2465.
7. Kunk, P.R., Bauer, T.W., Slingluff, C.L. et al. (2016). From bench to bedside a comprehensive review of pancreatic cancer immunotherapy. *J. Immunother. Cancer* **4**:14.
8. Evans, R.A., Diamond, M.S., Rech, A.J. et al. (2016). Lack of immunoediting in murine pancreatic cancer reversed with neoantigen. *JCI Insight* **1**:e88328. DOI:https://doi.org/10.1172/jci.insight.88328.
9. O'Reilly, E.M., Oh, D.-Y., Dhani, N. et al. (2019). Durvalumab With or Without Tremelimumab for Patients With Metastatic Pancreatic Ductal Adenocarcinoma: A Phase 2 Randomized Clinical Trial. *JAMA Oncol.* **5**:1431–1438.
10. Schmiechen, Z.C. and Stromnes, I.M. (2020). Mechanisms Governing Immunotherapy Resistance in Pancreatic Ductal Adenocarcinoma. *Front. Immunol.* **11**:613815. DOI:https://doi.org/10.3389/fimmu.2020.613815.
11. Balachandran, V.P., Łuksza, M., Zhao, J.N. et al. (2017). Identification of unique neoantigen qualities in long-term survivors of pancreatic cancer. *Nature* **551**:512–516.
12. Bailey, P., Chang, D.K., Nones, K. et al. (2016). Genomic analyses identify molecular subtypes of pancreatic cancer. *Nature* **531**:47–52.
13. Cristescu, R., Mogg, R., Ayers, M. et al. (2018). Pan-tumor genomic biomarkers for PD-1 checkpoint blockade-based immunotherapy. *Science* **362**:eaar3593. DOI:https://doi.org/10.1126/science.aar3593.
14. Poschke, I., Faryna, M., Bergmann, F. et al. (2016). Identification of a tumor-reactive T-cell repertoire in the immune infiltrate of patients with resectable pancreatic ductal adenocarcinoma. *OncoImmunology* **5**:e1240859. DOI:https://doi.org/10.1080/2162402X.2016.1240859.
15. Hanahan, D. and Weinberg, R.A. (2011). Hallmarks of cancer: the next generation. *Cell* **144**:646–674.
16. Hanahan, D. (2022). Hallmarks of Cancer: New Dimensions. *Cancer Discov.* **12**:31–46.
17. Pearce, E.L., Poffenberger, M.C., Chang, C.-H. et al. (2013). Fueling immunity: insights into metabolism and lymphocyte function. *Science* **342**:1242454. DOI:https://doi.org/10.1126/science.1242454.
18. Cham, C.M., Driessens, G., O'Keefe, J.P. et al. (2008). Glucose deprivation inhibits multiple key gene expression events and effector functions in CD8+ T cells. *Eur. J. Immunol.* **38**:2438–2450.
19. Chang, C.-H., Curtis, J.D., Maggi, L.B. et al. (2013). Posttranscriptional control of T cell effector function by aerobic glycolysis. *Cell* **153**:1239–1251.
20. Mockler, M.B., Conroy, M.J. and Lysaght, J. (2014). Targeting T cell immunometabolism for cancer immunotherapy; understanding the impact of the tumor microenvironment. *Front. Oncol.* **4**:107.
21. Buck, M.D., Sowell, R.T., Kaech, S.M. et al. (2017). Metabolic Instruction of Immunity. *Cell* **169**:570–586.
22. Michalek, R.D., Gerriets, V.A., Jacobs, S.R. et al. (2011). Cutting edge: distinct glycolytic and lipid oxidative metabolic programs are essential for effector and regulatory CD4+ T cell subsets. *J. Immunol.* **186**:3299–3303.
23. Bozza, P.T. and Viola, J.P.B. (2010). Lipid droplets in inflammation and cancer. *Prostaglandins Leukot. Essent. Fatty Acids* **82**:243–250.
24. Simons, K. and Ikonen, E. (2000). How cells handle cholesterol. *Science* **290**:1721–1726.
25. Yang, W., Bai, Y., Xiong, Y. et al. (2016). Potentiating the antitumour response of CD8(+) T cells by modulating cholesterol metabolism. *Nature* **531**:651–655.
26. Llaverias, G., Danilo, C., Mercier, I. et al. (2011). Role of cholesterol in the development and progression of breast cancer. *Am. J. Pathol.* **178**:402–412.
27. Scheinman, E.J., Rostoker, R. and Leroith, D. (2013). Cholesterol affects gene expression of the Jun family in colon carcinoma cells using different signaling pathways. *Mol. Cell. Endocrinol.* **374**:101–107.
28. Cruz, P.M.R., Mo, H., McConathy, W.J. et al. (2013). The role of cholesterol metabolism and cholesterol transport in carcinogenesis: a review of scientific findings, relevant to future cancer therapeutics. *Front. Pharmacol.* **4**:119.
29. Dimitrakopoulos, C., Hindupur, S.K., Häfliger, L. et al. (2018). Network-based integration of multi-omics data for prioritizing cancer genes. *Bioinformatics* **34**:2441–2448.
30. Lv, H., Liu, L., Zhang, Y. et al. (2010). Ingenuity pathways analysis of urine metabonomics phenotypes toxicity of gentamicin in multiple organs. *Mol. Biosyst.* **6**:2056–2067.
31. Saghafinia, S., Mina, M., Riggi, N. et al. (2018). Pan-Cancer Landscape of Aberrant DNA Methylation across Human Tumors. *Cell Rep.* **25**:1066–1080.e8.
32. Morgan, A.E., Davies, T.J. and Mc Auley, M.T. (2018). The role of DNA methylation in ageing and cancer. *Proc. Nutr. Soc.* **77**:412–422.
33. Bindea, G., Mlecnik, B., Tosolini, M. et al. (2013). Spatiotemporal dynamics of intratumoral immune cells reveal the immune landscape in human cancer. *Immunity* **39**:782–795.
34. Newman, A.M., Liu, C.L., Green, M.R. et al. (2015). Robust enumeration of cell subsets from tissue expression profiles. *Nat. Methods* **12**:453–457.
35. Zhu, Y., Ju, S., Chen, E. et al. (2010). T-bet and eomesodermin are required for T cell-mediated antitumor immune responses. *J. Immunol.* **185**:3174–3183.
36. Nicolle, R., Blum, Y., Marisa, L. et al. (2017). Pancreatic Adenocarcinoma Therapeutic Targets Revealed by Tumor-Stroma Cross-Talk Analyses in Patient-Derived Xenografts. *Cell Rep.* **21**:2458–2470.

37. Gros, A., Robbins, P.F., Yao, X. et al. (2014). PD-1 identifies the patient-specific CD8⁺ tumor-reactive repertoire infiltrating human tumors. *J. Clin. Invest.* **124**:2246–2259.
38. Speiser, D.E., Utzschneider, D.T., Oberle, S.G. et al. (2014). T cell differentiation in chronic infection and cancer: functional adaptation or exhaustion? *Nat. Rev. Immunol.* **14**:768–774.
39. Spear, S., Candido, J.B., McDermott, J.R. et al. (2019). Discrepancies in the Tumor Microenvironment of Spontaneous and Orthotopic Murine Models of Pancreatic Cancer Uncover a New Immunostimulatory Phenotype for B Cells. *Front. Immunol.* **10**:542.
40. Hingorani, S.R., Petricoin, E.F., Maitra, A. et al. (2003). Preinvasive and invasive ductal pancreatic cancer and its early detection in the mouse. *Cancer Cell* **4**:437–450.
41. Morton, J.P., Timpson, P., Karim, S.A. et al. (2010). Mutant p53 drives metastasis and overcomes growth arrest/senescence in pancreatic cancer. *Proc. Natl. Acad. Sci. USA* **107**:246–251.
42. Beatty, G.L., Chiorean, E.G., Fishman, M.P. et al. (2011). CD40 agonists alter tumor stroma and show efficacy against pancreatic carcinoma in mice and humans. *Science* **331**:1612–1616.
43. Gopinathan, A., Morton, J.P., Jodrell, D.I. et al. (2015). GEMMs as preclinical models for testing pancreatic cancer therapies. *Dis. Model. Mech.* **8**:1185–1200.
44. Barilla, R.M., Diskin, B., Caso, R.C. et al. (2019). Specialized dendritic cells induce tumor-promoting IL-10+IL-17+ FoxP3neg regulatory CD4+ T cells in pancreatic carcinoma. *Nat. Commun.* **10**:1424.
45. Zhang, Y., Zoltan, M., Riquelme, E. et al. (2018). Immune Cell Production of Interleukin 17 Induces Stem Cell Features of Pancreatic Intraepithelial Neoplasia Cells. *Gastroenterology* **155**:210–223.e3.
46. Gunderson, A.J., Kaneda, M.M., Tsujikawa, T. et al. (2016). Bruton Tyrosine Kinase-Dependent Immune Cell Cross-talk Drives Pancreas Cancer. *Cancer Discov.* **6**:270–285.
47. McAllister, F., Bailey, J.M., Alsina, J. et al. (2014). Oncogenic Kras activates a hematopoietic-to-epithelial IL-17 signaling axis in preinvasive pancreatic neoplasia. *Cancer Cell* **25**:621–637.
48. Zhang, Y., Yan, W., Mathew, E. et al. (2014). CD4+ T lymphocyte ablation prevents pancreatic carcinogenesis in mice. *Cancer Immunol. Res.* **2**:423–435.
49. Grover, S. and Syngal, S. (2010). Hereditary pancreatic cancer. *Gastroenterology* **139**:1076–1080.e10802.
50. Guerra, C., Schuhmacher, A.J., Cañamero, M. et al. (2007). Chronic pancreatitis is essential for induction of pancreatic ductal adenocarcinoma by K-Ras oncogenes in adult mice. *Cancer Cell* **11**:291–302.
51. Shi, X., Bi, Y., Yang, W. et al. (2013). Ca2+ regulates T-cell receptor activation by modulating the charge property of lipids. *Nature* **493**:111–115.
52. Gagnon, E., Schubert, D.A., Gordo, S. et al. (2012). Local changes in lipid environment of TCR microclusters regulate membrane binding by the CD3ε cytoplasmic domain. *J. Exp. Med.* **209**:2423–2439.
53. Molnár, E., Swamy, M., Holzer, M. et al. (2012). Cholesterol and sphingomyelin drive ligand-independent T-cell antigen receptor nanoclustering. *J. Biol. Chem.* **287**:42664–42674.
54. Zech, T., Ejsing, C.S., Gaus, K. et al. (2009). Accumulation of raft lipids in T-cell plasma membrane domains engaged in TCR signalling. *EMBO J.* **28**:466–476.
55. Kidani, Y., Elsaesser, H., Hock, M.B. et al. (2013). Sterol regulatory element-binding proteins are essential for the metabolic programming of effector T cells and adaptive immunity. *Nat. Immunol.* **14**:489–499.
56. Fraemohs, L., Koenen, R.R., Ostermann, G. et al. (2004). The functional interaction of the beta 2 integrin lymphocyte function-associated antigen-1 with junctional adhesion molecule-A is mediated by the I domain. *J. Immunol.* **173**:6259–6264.
57. Ostermann, G., Weber, K.S.C., Zernecke, A. et al. (2002). JAM-1 is a ligand of the beta(2) integrin LFA-1 involved in transendothelial migration of leukocytes. *Nat. Immunol.* **3**:151–158.
58. Yamada, A., Kaneyuki, T., Torimoto, Y. et al. (1992). Signaling from LFA-1 contributes signal transduction through CD2 alternative pathway in T cell activation. *Cell. Immunol.* **142**:145–158.
59. Jung, S.H., Yoo, E.H., Yu, M.J. et al. (2016). ARAP, a Novel Adaptor Protein, Is Required for TCR Signaling and Integrin-Mediated Adhesion. *J. Immunol.* **197**:942–952.
60. Ge, L., Wang, J., Qi, W. et al. (2008). The cholesterol absorption inhibitor ezetimibe acts by blocking the sterol-induced internalization of NPC1L1. *Cell Metab.* **7**:508–519.
61. Wang, Y., You, S., Su, S. et al. (2022). Cholesterol-Lowering Intervention Decreases mTOR Complex 2 Signaling and Enhances Antitumor Immunity. *Clin. Cancer Res.* **28**:414–424.
62. Ying, H., Kimmelman, A.C., Lyssiotis, C.A. et al. (2012). Oncogenic Kras maintains pancreatic tumors through regulation of anabolic glucose metabolism. *Cell* **149**:656–670.
63. Levine, A.J. and Puzio-Kuter, A.M. (2010). The control of the metabolic switch in cancers by oncogenes and tumor suppressor genes. *Science* **330**:1340–1344.
64. Ribas, A. and Wolchok, J.D. (2018). Cancer immunotherapy using checkpoint blockade. *Science* **359**:1350–1355.
65. Chambers, C.A., Kuhns, M.S., Egen, J.G. et al. (2001). CTLA-4-mediated inhibition in regulation of T cell responses: mechanisms and manipulation in tumor immunotherapy. *Annu. Rev. Immunol.* **19**:565–594.
66. Barber, D.F., Faure, M. and Long, E.O. (2004). LFA-1 contributes an early signal for NK cell cytotoxicity. *J. Immunol.* **173**:3653–3659.
67. Kristóf, E., Zahuczky, G., Katona, K. et al. (2013). Novel role of ICAM3 and LFA-1 in the clearance of apoptotic neutrophils by human macrophages. *Apoptosis* **18**:1235–1251.
68. Ediriweera, M.K. (2022). Use of cholesterol metabolism for anti-cancer strategies. *Drug Discov. Today* **27**:103347. DOI:https://doi.org/10.1016/j.drudis.2022.103347.
69. Zhou, J., Li, L., Wu, B. et al. (2024). MST1/2: Important regulators of Hippo pathway in immune system associated diseases. *Cancer Lett.* **587**:216736. DOI:https://doi.org/10.1016/j.canlet.2024.216736.
70. Sezgin, E., Levental, I., Mayor, S. et al. (2017). The mystery of membrane organization: composition, regulation and roles of lipid rafts. *Nat. Rev. Mol. Cell Biol.* **18**:361–374.
71. Gabitova-Cornell, L., Surumbayeva, A., Peri, S. et al. (2020). Cholesterol Pathway Inhibition Induces TGF-β Signaling to Promote Basal Differentiation in Pancreatic Cancer. *Cancer Cell* **38**:567–583.e11.
72. Li, J., Liu, J., Liang, Z. et al. (2017). Simvastatin and Atorvastatin inhibit DNA replication licensing factor MCM7 and effectively suppress RB-deficient tumors growth. *Cell Death Dis.* **8**:e2673. DOI:https://doi.org/10.1038/cddis.2017.46.
73. Tang, Z., Li, C., Kang, B. et al. (2017). GEPIA: a web server for cancer and normal gene expression profiling and interactive analyses. *Nucleic Acids Res.* **45**:W98–W102.
74. Huang, C.-S., Yu, X., Fordstrom, P. et al. (2020). Cryo-EM structures of NPC1L1 reveal mechanisms of cholesterol transport and ezetimibe inhibition. *Sci. Adv.* **6**:eabb1989. DOI:https://doi.org/10.1126/sciadv.abb1989.
75. Sen, M. and Springer, T.A. (2016). Leukocyte integrin αLβ2 headpiece structures: The αI domain, the pocket for the internal ligand, and concerted movements of its loops. *Proc. Natl. Acad. Sci. USA* **113**:2940–2945.

ACKNOWLEDGMENTS

This work was supported by the National Natural Science Foundation of China (Guideline-led Original Exploration Program Projects) (82150109), National Natural Science Foundation of China (82072745, 82273249, 81874211), National Postdoctoral Program for Innovative Talent (BX20200158), Science Foundation of Chongqing (2022NSCQ-MSX5088), Hospital Managed Fund Projects (SWH2016ZDCX1002), Natural Science Incubation Foundation of Chongqing University FuLing Hospital (flyygzkpy2022005, flyygzkpy2022004, flyygzkpy2022006) and The Natural Science Foundation of Chongqing (CSTB2023NSCQ-MSX0768). The funders had no role in study design, data collection and analysis, decision to publish, or preparation of the manuscript.

AUTHOR CONTRIBUTIONS

Conceptualization, J.O., H.L., Z.C., K.S., and X.L.; methodology, R.Z., K.S., X.S., P.Z., C.L., and Q.L.; investigation, R.Z., K.S., P.Z., X.S., Y.Y., Y.C., H.D., Y.L., H.M., W.W., and H.S.; visualization, K.S., Y.Y., L.W., R.Z., C.M., C.L., W.L., S.Z., and H.S.; funding acquisition, J.O., H.L., Z.C., P.Z., H.D., K.S., W.W., H.M., and X.L.; project administration, J.O., H.L., Z.C., and P.Z.; supervision, J.O., H.L., Z.C., and X.L.; writing – original draft, J.O., R.Z., K.S., X.S., P.Z., and Y.Y.; writing – review & editing, J.O., H.L., Z.C., X.L., R.Z., and K.S. All authors contributed to and approved the manuscript.

DECLARATION OF INTERESTS

The authors declare no competing interests.

SUPPLEMENTAL INFORMATION

It can be found online at https://doi.org/10.1016/j.xinn.2024.100783.